COMPARISON OF DIFFERENT METALS AS ELECTRODES FOR A FLEXIBLE MICRO pH SENSOR

by

PAVAN KUMAR KOTA

Presented to the Faculty of the Graduate School of

The University of Texas at Arlington in Partial Fulfillment

of the Requirements

for the Degree of

MASTER OF SCIENCE IN ELECTRICAL ENGINEERING

THE UNIVERSITY OF TEXAS AT ARLINGTON

May 2016

This thesis is dedicated to my grandfather Late Mr. K.V. Subrahmanyam whose knowledge and wisdom will always be my driving force.

I would also like to dedicate this thesis to my mother and father.

ACKNOWLEDGEMENTS

First and foremost, I would like to express my deepest appreciation and gratitude to my supervising professor Dr. Jung-Chih Chiao for his continuous guidance, encouragement and support throughout my Master's degree program. I want to thank Dr. Chiao for believing in my abilities, giving me an opportunity to work on interdisciplinary projects and guiding me throughout the process. I feel fortunate to have access to iMEMS laboratory's equipment and resources which enabled me complete my research. Without the support of Dr. Chiao, this thesis wouldn't have been possible. I am also grateful to Dr. Weidong Zhou and Dr. Yuze (Alice) Sun and would like to thank them for taking interest in my research and accepting to serve on my committee.

I am thankful to Dr. Smitha Rao for guiding me in the initial days of my research to get acquainted with the methodology of research. I would also like to express my deepest gratitude to Dr. Cuong Manh Nguyen for being a good friend and also a great guide. I would also want to thank Mr. Souvik Dubey, Mrs. Xuesong Yang and Mr. Nguyen Quoc Minh for supporting me throughout my research and for being such great friends. I also thank the staff at UTA Nanofab and Dr. Hozhabri for providing an excellent clean room facility to carry out my research.

Most importantly, I would want to extend my heartfelt appreciation and gratitude to my father Mr. Purushotham Kota, my mother Mrs. K.V. Surya Ratnam and my sister Ms. Madhuri Kota who always believed in me and supported me throughout the journey.

Finally, I would want to thank God Almighty for giving me strength and determination to complete my research.

April 6, 2016

ABSTRACT

COMPARISON OF DIFFERENT METALS AS ELECTRODES FOR A FLEXIBLE MICRO pH SENSOR

PAVAN KUMAR KOTA, MS

The University of Texas at Arlington, 2016

Supervising Professor: Dr. Jung-Chih Chiao

pH can be explained in general terms as a numerical scale used to state the acidity or basicity of an aqueous solution. Keeping track of pH is very useful in many applications like medicine, civil engineering, chemical engineering, biology, water purification etc. Most commonly used pH sensors employ glass electrodes but there are some disadvantages associated with these kinds of pH sensors. Glass is a rigid, chemically reactive and fragile material. Also, glass electrodes, owing to the size require significant quantity of solution to test for pH which makes it difficult to use in cases where we have very little quantities of the solution to be tested (say, milliliters). In addition, the sluggish response and requirement for a high input impedance pose a challenge for accurate pH measurements and thereby force us to look for a better alternative.

Currently the research in this field points to a flexible micro pH sensor which employs Gold as one of the electrode with an Iridium Oxide (IrO_x) sensing film and another Ag/AgCl reference electrode. The potential difference between these two electrodes can be used to

calibrate the device and measure the pH of the solution. This method offers solution to many existing problems like flexibility, size of the sensor, fragile nature of the glass electrode etc.

In this work, we have demonstrated the ability to use other metals as material of choice to replace Gold as an electrode in the existing flexible micro pH sensor. In addition, the effect of using different adhesion layers for these metal thin films is also tested and the pH sensing ability of all these materials are compared to the Gold electrode-IrO_x thin film based pH sensor. We have used a commercial Ag/AgCl electrode as a reference. Nickel (Ni) and Aluminum (Al) in conjuncture with different adhesion layers like Chromium (Cr), Titanium (Ti) and Carbon (C) have been used as the alternative for Gold. Hence, we have significantly reduced the cost of pH sensor by replacing Gold with other metals to fabricate pH sensors which can be used in applications such as soil testing, water purity testing etc., which do not need a Gold electrode based pH sensor.

The fabrication process includes metal deposition for electrodes, patterning, sol-gel coating and its thermal oxidation to form IrO_x sensing film. This IrO_x film has been characterized using scanning electron microscope (SEM) and electron dispersive analysis (EDAX). The sensors' characterization and performance have been probed into, making note of many parameters like sensitivity, stability, reversibility and repeatability. The results are compared with Gold electrode based pH sensor. These sensors have shown encouraging sensing performance in the pH ranges of 2 to 12 in the case of Al based pH sensors and 4 to 10 in the case of Ni based sensors with a near-Nernstian response at 25^o C. The sensors have been tested using standard buffer solutions with foreknown pH values.

In conclusion, the flexible IrO_x pH sensor mentioned in this thesis can be used for sensing applications where small spaces and curved surfaces pose problems to a traditional glass electrode based sensor. They also gives a significant cost reduction when compared to gold electrode based flexible pH sensor.

TABLE OF CONTENTS

LIST OF ILLUSTRATIONS

LIST OF TABLES

CHAPTER ONE: INTRODUCTION

1.1 Motivation

Since the inception of the concept of pH in 1909, measuring pH of solutions has become essential for many applications like food, chemical and bio-material industries. pH can be measured by different means but using two different electrodes and measuring potential difference between them when placed in a solution and calibrating the device to accurately reveal the pH of that solution started as an idea in the 1920s. Developing on this idea, Dr. Beckman registered a patent for a 'first of its kind' pH measuring chemical instrument and named it 'acidimeter' [1]. The patent was formally accepted in October, 1934.

1.2 Proposed Approach

We are more interested in using a flexible micro-scale pH sensor for many application. The different kinds of pH sensors currently being used which can be miniaturized and have a robust design are optical fiber pH sensor [2, 3-8], solid state pH sensors [9-12], hydrogel film pH sensor [13-15] and ion-sensitive field effect transistor (iSFET) pH sensors [1, 16-19]. The optical pH meter consumes power owing to the light source present in the device. The fabrication procedure employed in a hydrogel based sensor is complex and adds cost to the process. Similar to the optical fiber pH sensors, the iSFET pH sensor also consumes a lot of power. There has been innovation into metal-oxide based pH sensor which employs an electrode which has an overlaying metal-oxide sensing film and another reference electrode. The potential difference between the two electrodes is measured when the device is placed in the buffer solution of unknown pH. Based on this potential difference, the pH can be obtained.

This type of pH sensor has many advantages over other pH sensors that were mentioned in the beginning of this section because of the simplicity in fabrication, cost effectiveness and low power consumption. Especially, we have one particular type of metal oxide based pH sensor which uses an IrO_x film (IROF). This metal oxide can be deposited onto a conducting electrode using many thin film deposition methods but the current method uses an inexpensive process of coating the electrode with sol-gel by dipping in the solution followed by drying the electrode and later using thermal treatment to oxidize the Iridium based compound in the sol-gel coating to form IrO_x film. The process of sequential heat treatment of sol-gel to form an amorphous IROF [25] has been frequented by the industry. This is highly cost effective and gives better quality of IrO_x sensing film [20].

1.3 Innovation

In order to obtain cost effectiveness and also to simplify the fabrication process we can use a metal-oxide based pH sensor. There are several solid state metal oxides that can be used for this purpose like PtO_2, IrO_x, RuO_2, OsO_2, Ta_2O_5, RhO_2, TiO_2 and SnO_2 [9]. Of these IrO_x, RuO_2 and SnO_2 have shown better pH sensing capabilities [21]. However SnO_2 and RuO_2 have drift and hysteresis problems leading to unstable responses and calibration problems [22, 23].

Literature review shows that IROF has edge over other metal oxides to use it in pH sensing applications because of the stability, rapid response and low potential drift [24]. Also, there is an existing pH sensor fabricated using IROF formed from thermal treatment of sol-gel which has been coated onto the metal (Gold) electrode. The potential is measured between this electrode and an Ag/AgCl reference electrode. In many applications like water purity testing, soil analysis etc. employing gold as the metal electrode may prove to be expensive.

In this work, we tried to investigate the possibility and effectiveness of using different metals as the materials of choice to fabricate the electrode on a flexible substrate and the performance was compared to that of the existing Gold-IROF based pH sensor. Also, the effect of different adhesion layers is tested and the results are compared. We have discussed design, fabrication, characterization and testing of the flexible micro pH sensor.

1.4 Thesis Organization

This thesis is divided into three parts. The first part which includes chapter 2 and 3 deal with the fabrication and characterization of the flexible micro pH sensor. Chapter 2 deals with literature review of iridium oxide, preparation procedure and its use as a pH sensing material. It also emphasizes on different metals that can be used as electrodes for a micro scale IROF based pH sensors. Chapter 3 gives us an overview of the fabrication of electrodes using different metals followed by sol-gel coating and thermal treatment methods to form IrO_x sensing film.

The second part of the thesis includes chapter 4, wherein, we see the detailed fabrication process which is followed by characterization of the sensing area of the devices using SEM and EDAX.

The third part includes chapter 5 which gives us an understanding of the testing methodology used and the results obtained. Here, we tested the sensor in standard pH buffer solution and the results obtained for each type of the sensor are compared to the Gold electrode-IROF sensor. The parameters like sensitivity, repeatability and reversibility are obtained and compared. Observations and made and the results are discussed.

CHAPTER TWO: LITERATURE REVIEW

2.1 Iridium and Iridium Oxide (IrO_x)

Iridium (Ir) is a transition metal and also a noble metal, which means that it is not affected by different pH levels or the surroundings. This implies that Ir has high resistance to react to some of the highly alkaline or acidic reagents and oxidizing agents [26]. Iridium is highly corrosion resistant and studies show that it stays stable up to temperatures as high as 2000^o C. Iridium is also expensive in its purest state. Ir most commonly exists in the +3 and +4 oxidation states as Ir_2O_3 and IrO_2. The formation of different oxides of Ir can be explained as follows. Heating Ir in the presence of air results in IrO_2 which tarnishes the Ir. When Ir is heated to a temperature of 750-1000^o C, IrO_4 is formed. Ir_2O_3 generally exists as hydrated oxide. The anhydrous form is usually difficult to prepare. The Iridium (III) oxide exists as $Ir_2O_3.xH_2O$ which is soluble in chemical reagents like alkalis and acids resulting in oxidization by regular oxidizing agents like air to form Ir (II) of $IrO_2.2H_2O$.

Therefore, different types of Iridium oxide (IrO_x) can be formed by the oxidation of Iridium under different conditions. The physical and chemical properties of the IrO_x are dependent on the structure and composition which in turn depends on the fabrication method employed to form the oxide. One of the most stable oxides of Iridium is IrO_2 and the crystal lattice structure is shown in Figure. 1. IrO_2 crystallizes into a tetragonal rutile structure [27]. The rutile structure contains octahedral coordination of metal ions which are shred at the edges and form chains along the [001] direction. In a rutile structure, the O−O bonds are not of equal bond length, so the base of the octahedron is not symmetric, because of the fact that the shared edge is shorter than the edge parallel to the c axis.

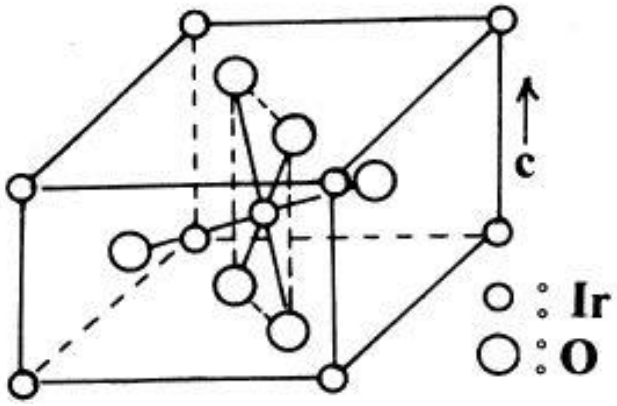

Figure 1: The crystal structure of a unit cell of a tetragonal IrO_2 [27]

IrO_x formation can be accomplished by both thermal and electrochemical methods. Anodic iridium oxide film (AIROF) can be obtained by electrochemical fabrication. The highly hydrated surface and poorly crystallized structure are the main attributes of these kinds of iridium oxide films [21]. Sputtering iridium oxide film (SIROF) and sol-gel (SG) based IrO_x film are based on thermal method. In SG based IROF, we employ oxidation through annealing in the fabrication process. The different heating profile and temperature points will change the morphology of the iridium oxide [28]. The difference in structure is a crucial phenomenon which can be used in different applications. For example, the highly crystalline IrOx structures enhance the electro-chromic properties such as light dispersion and can be used to improve the absorption in the solar cell for energy harvesting applications [28]. The stability and quality of the surface is controlled by the crystallization of the constituent atoms. For pH sensing applications, a stable sensing film of IrOx is required. Less crystalline structures are physically stable in which the iridium atom is aligned and stacked in the same order. The structures with higher crystalline nature contain more disordered iridium oxide atoms. Hence, in crystalline

structures with higher crystallization, the atoms are loosely packed which is not good for long term sensing applications.

Now that we have an idea about the IrO_x, we will look into different ways of fabricating one to obtain the desired crystal structure so that it can be used in pH sensing applications.

2.2 Techniques to deposit IrO_x film

2.2.1 *Sputtering*

Depositing IrO_x through the process of sputtering is used more often and gives an amorphous film. The cost of the target makes this process very costly. At room temperature, the SIROF has a distinctive rutile pattern from films deposited at 200ºC or more. In general, a good film quality is obtained from depositing at very slow rates (<2 nm/min). The sputter rate can be adjusted by different parameters of the sputtering machine such as the oxygen and argon pressure ratios, relative position of the target and RF power during the fabrication processes. The quality of the sensing film affects the pH sensing parameters such as potential drifts and redox interferences [21].

2.2.2 *Electrodeposition*

In this process, the IrO_x film can be deposited on a conducting electrode like Platinum (Pt), Titanium (Ti) etc. There is no need for an Ir substrate which means that the cost is reduced when compared to other methods. There has been research where IrO_x film was electrodeposited on Indium Titanium Oxide (ITO) conducting polymer using Iridium Chloride, hydrogen peroxide, Potassium carbonate and Oxalic acid as a precursor. A current of 2-3 A/m^2 is driven into cathode or anode at 10^0 C for 15 minutes. Deposition in such a case is affected by the properties of the deposition solution like pH, temperature etc. and also the

current density [29] which means that the IROF quality is highly dependent on many factors. This results in a film which is not highly reliable and can have varying results when used for pH sensing.

2.2.3 *Thermal Oxidation*

Thermal treatment of pure Ir can leads to oxidation and formation of Iridium Oxide. Research shows that oxidation in Ir takes place at around 800^0 C [30]. This results in an anhydrous oxide film which is similar in properties with the SIROF. The main problem associated with the thermal treatment, though it leads to a good quality oxide film, is that high temperatures are used. During high temperature treatment, the oxide film that is formed can crack. Also the substrate must be chosen in a way so that it can withstand the temperature. All these factors constraint us into choosing specific materials and also lead to an unstable oxide film because the cracks on the oxide film may cause adhesion problems. It is also worth mentioning that pure Ir is highly expensive and hence makes the process very costly.

2.2.4 *Thermal deposition using Sol-gel (SG)*

Sol-gel IROF is formed when the sol-gel is 'dip-coated' and treated by sequential thermal process resulting in an IrO_x film [28, 31-32]. Iridium Chloride ($IrCl_4$) has been used as a starting material for the sol-gel dip coating process. The solution is formed by mixing Iridium Chloride, ethanol and acetic acid. Using the metal electrode withdrawal rate of 2.0 cm/min from the sol-gel solution and a heat treatment at 300^0 C, an oxide film with no impurities is formed. Crystallization takes place over 450^0 C which means that by controlling the temperature and dip rate we can control the quality of IROF as desired. The factors like

dip coating and low temperature treatment make sol-gel thermal deposition of IROF economical and reliable.

2.3 IrO_x: Mechanism of pH sensing

There have been five electrode mechanism formulated for the metal oxides:

- Ion exchange on the surface layer which contains OH^- groups. This mechanism is common to the glass electrode.
- A redox equilibrium between a lower and a higher valence oxide or an oxide and a pure metal.

  For example, the Antimony (Sb) electrode:

$$Sb_2O_2 + 6\ H^+ + 6\ e^- \rightleftharpoons 2\ Sb + 3H_2O$$

- pH dependent potential can also be created in some cases by a steady state corrosion of the electrode material
- A redox equilibrium involving a solid phase whose hydrogen content can be varied on continuous basis by passing an electric current through the electrode. This type of a reaction is termed as an intercalation reaction. A general scheme for the above mentioned reaction is as follows:

$$H_xMO_n + y\ H^+ + y\ e^- \rightleftharpoons H_{x+y}MO_n$$

- Similarly, an intercalation reaction involving oxygen can also be described. Anyhow, there has been no examples of pH sensing mechanism involving such a reaction.

Hence, for Iridium based oxides three mechanisms have been proposed for a pH dependent redox intercalation equilibrium. This equilibrium is between two different oxidation states of iridium oxide [33].

$$Ir_2O_3 + 6\ H^+ + 6\ e^- \rightleftharpoons 2\ Ir + 3\ H_2O \qquad (1)$$

$$IrO_2 + 4\ H^+ + 4\ e^- \rightleftharpoons Ir + 2\ H_2O \qquad (2)$$

$$2\ IrO_2 + 2\ H^+ + 2\ e^- \rightleftharpoons Ir_2O_3 + H_2O \qquad (3)$$

$$E = E^0 + 2.303\left(\frac{RT}{F}\right) pH = E^0 \pm 0.05916\ pH \qquad (4)$$

E^0 is a constant called the standard electrode potential which is a reference potential and depends on the reference electrode of choice. For a standard hydrogen electrode the value of E^0 is 926 mV and for an Ag/AgCl reference electrode this value is 577 mV. The value of $\left(\frac{RT}{F}\right)$ is approximately 25.69 at 25^0 C as R is the gas constant which is 8.314 J/deg and F is the faraday's constant with a value of 96,487 C/eq.

For a Nernstian response, the pH potential sensitivity is at -59 mV/pH [21, 33-34]. For most of the sensors that will be discussed in further chapters, the intercept at pH=0 gives a potential of the range of 550 mV to 630 mV with respect to the reference electrode which close to the theoretically expected value mentioned above. Although there is theoretical estimate of the expected relative potential between the electrode and the reference, this value is bound to change when we use different electrodes. This is because of the simple fact that the

stoichiometry of oxide compound and oxidation states of Iridium oxide change [21]. Hence, we have different values for the intercept at pH=0 for different metals.

2.4 Different metals as electrodes in pH sensors

The most stable metal that can be used as an electrode for pH sensing application is Au as it is a noble metal. Au doesn't react easily with the atmosphere or other reagents. Therefore, it stays stable in the entire testing process. It is not affected by highly acidic and alkaline solutions. Au with an adhesion layer of Cr and a thin IROF on the surface can be used as a pH sensor. It has been demonstrated that a sensitivity of -77 mV/pH is obtained by using the Cr-Au thin film on a flexible substrate [40-42].

We can also use different metals as electrodes for a pH sensor. As discussed above, they might each behave differently which means that their responses and sensitivities can be different for a given solution for which the pH needs to be tested. There has been research into using different metals as an electrode for a pH sensor while keeping the reference electrode fixed. Firstly, in [35, 38], discussion about using a platinum electrode with IROF as a pH sensor is presented. The precursor is the same which is used in the current research. This device has a good pH sensing capability to this sensor with a sensitivity of -77.6 mV/pH. To fabricate the device, a thin film of Ti is used as an adhesion layer and Pt is deposited on this layer. This device is not flexible as the substrate chosen is glass. When this device is transferred on to a flexible substrate there is a possibility of reduced performance [37]. It is observed that the sensitivity drops to -63.5 mV/pH. Also, Pt is a costly material and hence doesn't fit into our research towards finding a cheaper alternative.

In another research presented in [36], an etched metal substrate like Ti is used and IrO_x is deposited onto this substrate. This device, when tested for response towards pH resulted in a sensitivity of around -73 mV/pH. In addition, a variety of pure metals like Au, Ag, Ti, Cu, Ni etc. were tested. Although the sensitivities were good to use them as pH sensors, these results might not hold in case of metallic thin film on flexible substrate. For a metallic thin film, there are many factors that may change the sensitivity like oxide formation, reaction towards reagents etc. For the purpose of testing, a metal is chosen from this lot which can replace Gold as an electrode for pH sensing applications.

There are many other substances that have been used in conjuncture with an IrO_x thin film so that the device can be used for pH sensing applications. Some of them include Tin-doped indium oxide (ITO), W, Zr, Co, Stainless steel, SnO_2 coated glass etc. and all of the devices thus formed have sensitivities in the range of 68 to 75 mV/pH [39].

In this research, the metals are chosen keeping these approaches and results in mind and the sensitivities are compared for different adhesion layers used for the given metal. While performing this, the cost factor is also taken into consideration so that the metal that is assured to be a good pH sensing material can replace gold, thereby, reducing the cost of the device on the whole.

2.5 Discussions

The physical properties, fabrication method and pH sensing mechanism of IrO_x thin film are reviewed. In addition, a discussion is made on different metals that have been used by other researchers for the purpose of pH sensing. Taking a cue from these, we can zero in onto a

particular methodology that can be employed for the fabrication and testing of pH sensors. We know that, low crystalline IrO_x film has stable and better pH sensitivity. The substrate is chosen to be flexible which means that we would need to employ low temperature thermal annealing process. Keeping these aspects in mind, we have chosen the sol-gel process to fabricate the sensors. Sol-gel process has many advantages including low cost and high reliability. Now that we have chosen the process, the metal to be used to fabricate the electrode needs to be decided upon. In the previous section many metals have been discussed. But to ease the fabrication process and to keep the cost low, we choose electrode made from metals like Nickel which can be fabricated easily. The numerical value of sensitivity judges the performance of the sensor. Any sensor with a lower sensitivity would mean that there is a structural flaw in the film of either the electrode or the IROF. IROF that is porous or that has cracks can give a lower sensitivity.

The next chapter deals with fabrication and characterization of the sensor.

CHAPTER THREE: SENSOR FABRICATION PROCESS

3.1 Overview

There are three major steps in the fabrication process of the pH sensor. These steps are enlisted below:

- Fabrication of the metal electrode
- Sol-gel process
- Fabrication of Ag/AgCl reference electrode

To fabricate a metal electrode on a flexible substrate we can use lift-off or etching. To make the fabrication simpler, we make use of the lift-off process. In the lift-off process, the photoresist is spun on the substrate to obtain the desired thickness. The photoresist is patterned by exposing and developing. Subsequently, metal deposition is done on the substrate by using either sputtering or e-beam evaporation. During metal deposition we can also deposit an adhesion layer before depositing the metal. When a conformal layer of metal is deposited of the desired thickness, we place the sample in acetone so as to strip the photoresist. When the photoresist is stripped, the metal is also removed and the patterned electrode structure is left behind on the substrate. To obtain a conformal and good electrode pattern, we need to keep a lot of aspects in mind.

Firstly, the substrate should be clean. In general, we employ the cleaning methodology depending on the substrate of choice. Here, we used kapton as a substrate, and hence we made use of the appropriate cleaning method. Secondly, the photoresist needs to be spun on evenly and temperature needs to be precise for the pre-bake process. Next, we need to expose and

develop for precise time duration. Also, the metal deposition rate must be optimal to form a conformal metal deposition. Since, we have metal thin film, the lack of conformity can pose severe issues.

At the end of the lift-off process, we get the metal electrode on which the sol-gel process is performed to deposit a thin film of IrO_x. During sol gel process the entire electrode, except the sensing area, is covered with an SU-8 sacrificial layer. The electrodes are dipped into the sol-gel to expose the sensing pads to the solution. After the sol-gel dries up, the SU-8 layer is removed and a sequential thermal treatment is performed to oxidize the precursor containing Ir to obtain a thin film of IrO_x on the sensing area of the metal electrode. To expose just the sensing area to the solution for which the pH is to be tested, we insulate the rest of the electrode using photoresist. This is a virtual device packaging and protects the device from any external influence.

There is also another important process involved which is the fabrication of Ag/AgCl reference electrode on the flexible substrate alongside the metal electrode. We use regular micro-fabrication techniques to fabricate the silver electrode and then use electro-deposition to form a layer of AgCl on the electrode. This acts as a reference electrode. Though the fabrication methodology is discussed in this thesis, we used a standard commercial reference electrode of Ag/AgCl to reduce the complexity of the fabrication.

A schematic depicting the fabrication methodology is shown in Figure 2. This method is employed in [41] to fabricate the sensors. Though the method employed is same with the fabrication methodology followed in this thesis, there are certain differences.

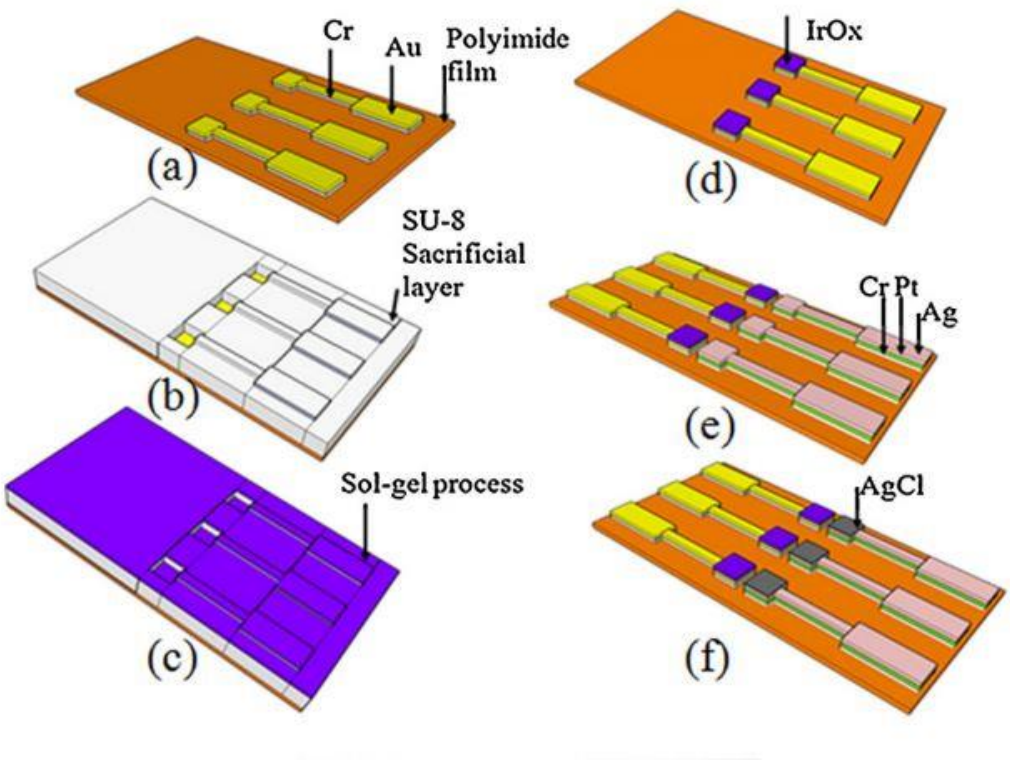

Figure 2: Flow to fabricate a flexible micro-pH sensor which has a metal electrode along with an IrO_x thin sensing film and a reference Ag/AgCl electrode [41]

The sol-gel process and Ag/AgCl reference electrode fabrication are discussed now. These processes remain common for all the metals.

3.2 IrO_x film formation: The sol-gel process

At first, we will discuss about the coating agent which is used as a precursor for introducing Ir based compound onto the sensing area. The coating agent must have an Ir based compound which on thermal treatment oxidizes to form IrO_x. This compound could be in solid state which means that we need to have a solvent that is used as a carrier for the Ir based compound. The solvent needs to dry up quickly to ease the process.

The process that takes care of all these aspects is introduced in [31] meant for rigid surfaces. The process involved one gram of anhydrous iridium chloride ($IrCl_4$) dissolved in a solution which is essentially a mixture containing 42 ml of ethanol (C_2H_5OH) and 10 ml of acetic acid (CH_3COOH). The solution thus formed was continuously mixed with a magnetic stirrer for at least an hour.

This sol-gel, upon thermal treatment, oxidizes the $IrCl_4$ to form IrO_x. The chemical reaction that describes the process is shown below:

$$2\ IrCl_4 + 3\ H_2O \xrightarrow{300^0\ C} Ir_2O_3 + 6\ HCl + Cl_2$$

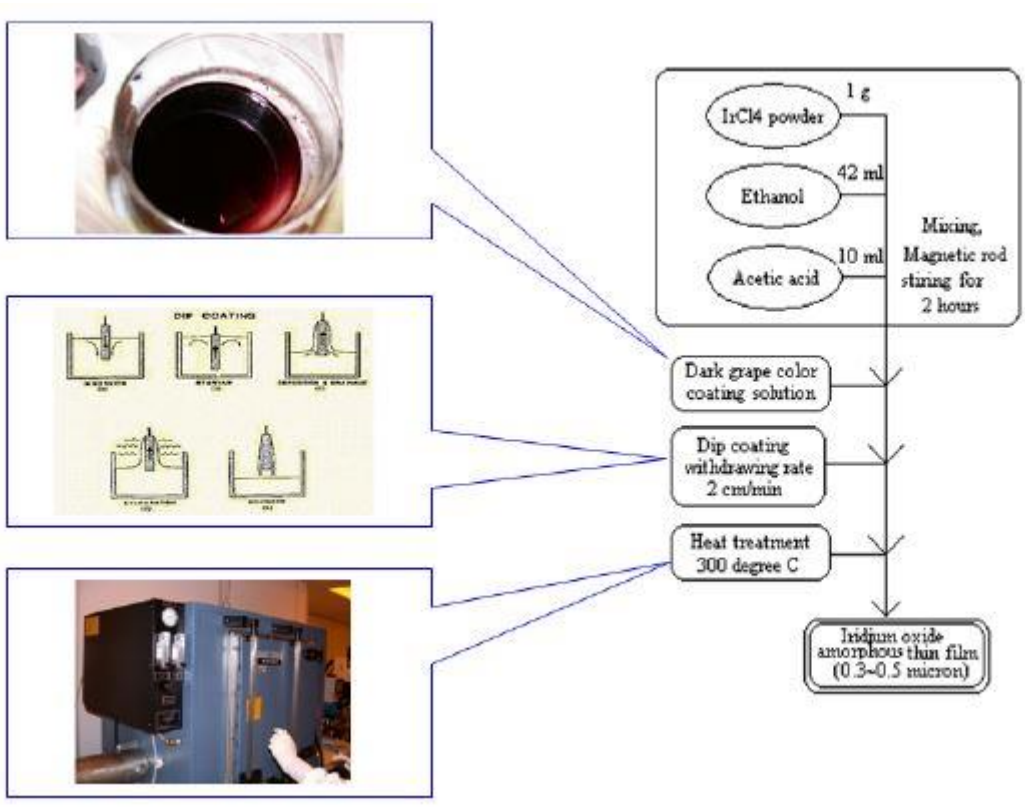

Figure 3: Schematic of sol-gel coating and thermal treatment [42]

The main reason to choose dip coating is that when $IrCl_4$ is dissolved into ethanol, the former just floats on the surface of the solution. When we use dip coating more $IrCl_4$ particles are condensed onto the substrate which increases the thickness and conformity of the IrO_x film. Therefore, dip coating is preferred when compared to spin or spray coating.

Acetic acid is added to keep the pH at a low level so that there are no unnecessary chemical reactions taking place in the solution [31].

The schematic diagram for sol-gel process is presented in Figure 3.

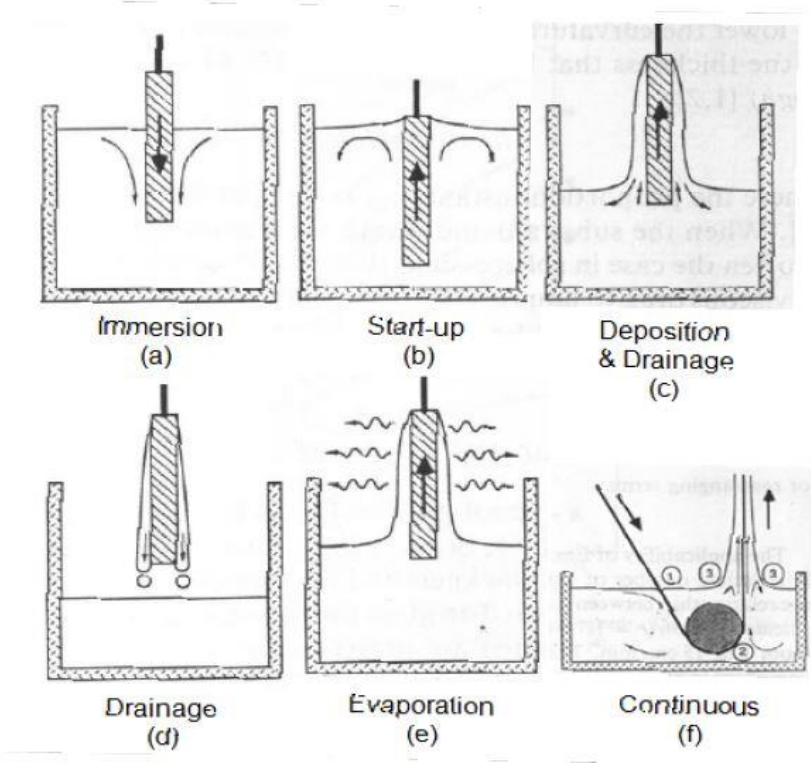

Figure 4: Six stages of dip coating process

A detailed experimentation on the procedure needed to be followed for the dip coating process is presented in [42] and it turns out that to obtain higher sensitivity we need to withdraw the sample from the sol-gel solution at a rate of 10 cm/min. At higher withdrawal rate, the

thickness of the IrO_x increases but the sensitivity reduces after a while. Dip coating has been clearly depicted in [32] showing different phases involved in the dip coating process. This gives us an idea as to what process needs to be followed. The process flow is shown in Figure 4. As the electrode's sensing area is now coated with sol-gel, the SU-8 layer that is used as protective coating to stop the sol-gel from reaching the other parts of the sensor is removed using a tweezer. As the substrate is flexible, it is very easy for us to perform the task.

The next step is the annealing process in which we subject the sol-gel coated electrode through a sequence of thermal treatment. The resultant film must be an amorphous and stable. There is research into different temperature treatments and the resultant IROF quality which is presented in [42]. The annealing temperature has thus been narrowed down to the range of 300^0 C to 350^0 C. At higher temperatures, it has been observed that the IrO_x thin film formed has cracks on its surface which will deteriorate the performance of the sensor over a period of time.

3.3 Ag/AgCl reference electrode

Ag is deposited on the kapton substrate using electron beam evaporation and patterned similar to the metal electrode. To plate the silver electrode with AgCl electrochemical anodization is availed in which the silver electrode which acts as an anode is placed in 0.1M HCl along with a platinum cathode. A current of 0.5 mA is applied to the electrodes which results in a brown colored layer of AgCl on the surface of Ag electrode. The reference electrode is thus formed and is then cleaned with DI water. Then, in the next step, the electrode is immersed in 3M KCl solution for 24 hours to saturate and stabilize potentials [43].

For the current research we have used a commercially available Ag/AgCl electrode to make the fabrication simpler.

3.4 Conclusion

The process involving the formation of metal electrode is discussed. After the formation of metal electrode a layer of SU-8 is spun on the substrate and a window is created at the sensing region so as to expose the area and perform the sol-gel process on it. Sol-gel dip coating process is discussed and optimal withdrawal time is confirmed from literature. After the dip coating process, the substrate is dried up and the protective SU-8 layer is peeled off using a tweezer. Subsequently, the substrate with the electrode and sol-gel coating is subjected to a sequential thermal treatment which oxidizes the Ir compound in the sol-gel to give us IrO_x thin film. An insulating coating is used to expose just the sensing area so that there is no interference between the test reagent and the electrode.

CHAPTER FOUR: MATERIAL SPECIFIC FABRICATION AND CHARACTERIZATION

4.1 Nickel electrode based IROF pH sensor

4.1.1 Nickel thin film electrode with no adhesion layer

Our initial material of choice to fabricate the electrode was Nickel (Ni). First let us look at the process employed for the fabrication of the electrodes. We took a 125 micron kapton and cleaned it according to standard cleaning procedure so that there are no dust particles on the substrate. Once it is confirmed that the substrate is good to be used, we spun a positive photoresist on the substrate to obtain uniform coating and then pre-exposure bake was performed. We used a dark field mask and exposed it to UV light for specific time duration and developed it.

The resultant pattern contains photoresist on the regions which does not form a part of the electrode. This means that, after lift-off we are left with metal deposited in the region where the electrode is expected.

We used e-beam evaporation to deposit Ni using Ni pellets with a purity of 99.95 % and at a deposition rate of 1-1.5 A/s. After the deposition was done, the substrate was placed in a bath containing acetone and was agitated gently so that the photoresist along with the metal on top of it is stripped away leaving the metal patterned in the desired way on the substrate. The samples were then cut from the substrate to ease the process of SU-8 coating and sol-gel treatment.

It was then required to cover the entire electrode barring the sensing area so that sol-gel treatment can be done. For this purpose, we needed a thick protective coat that could be peeled off after the process. We chose SU-8-100 which gives a pretty thick coating and can also be peeled off very easily.

After this, the sol-gel dip coating process was accomplished and the SU-8 layer was peeled off. To form the IROF, the sequential thermal treatment, which was mentioned in the previous chapter, was performed.

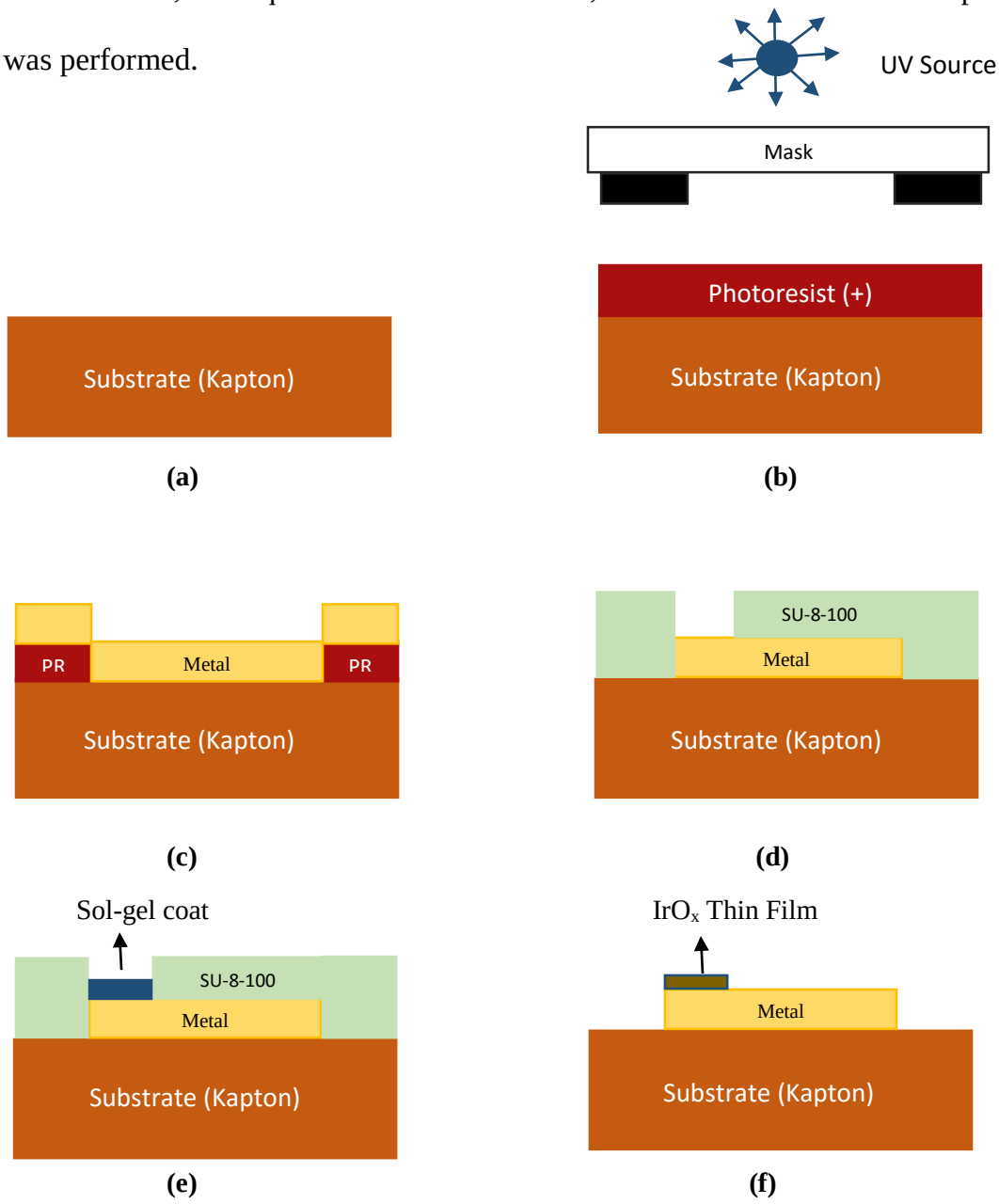

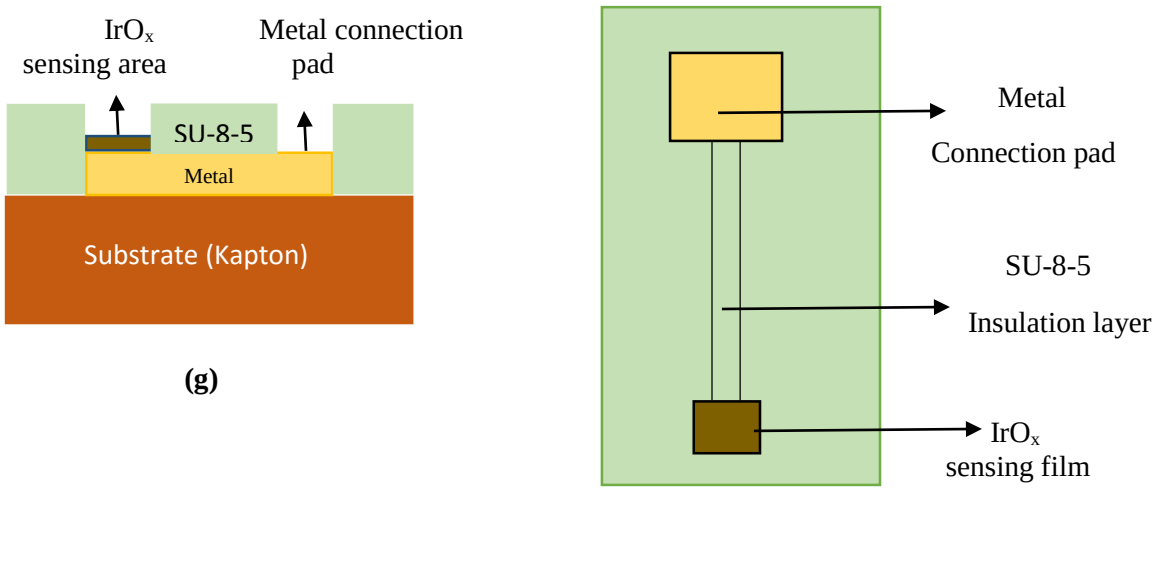

Figure 5: (a) A clean kapton substrate is chosen (b) Photoresist is spun, pre exposure bake, exposure and development is performed (c) Metal deposition (d) PR stripping using acetone, SU-8-100 spin coating and patterning (e) Sol-gel dip coating, SU-8-100 layer peel off and sequential thermal treatment (f) IrO_x thin film formation (g) insulating the device with SU-8-5 just to expose the sensing area and metal connection pad (h)Top view of the sensor with sensing area of 1mm x 1mm.

Then, SU-8-5 was used to create an insulation so that there is no interference between the other parts of the metal electrode and the pH buffer solution during the sensitivity test. The fabrication process is shown in Figure 5 where in the metal is Ni.

Figure 6 shows the SEM of the Ni-IROF based pH sensor. To understand the surface composition of the sensing area, we can make use of Energy Dispersive X-ray Spectroscopy (EDAX). The EDAX for the sensing area of the Ni-IROF pH sensor is presented in Figure 7.

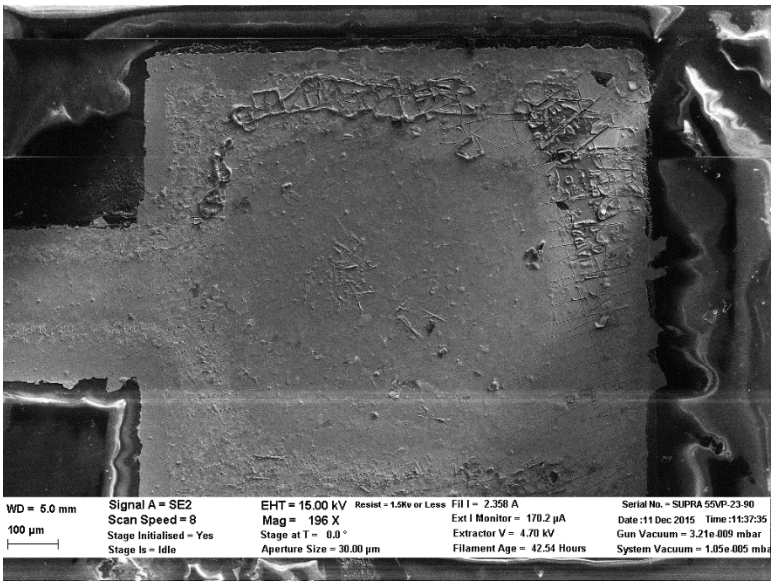

Figure 6: SEM of the sensing area of the Ni electrode-IROF pH sensor

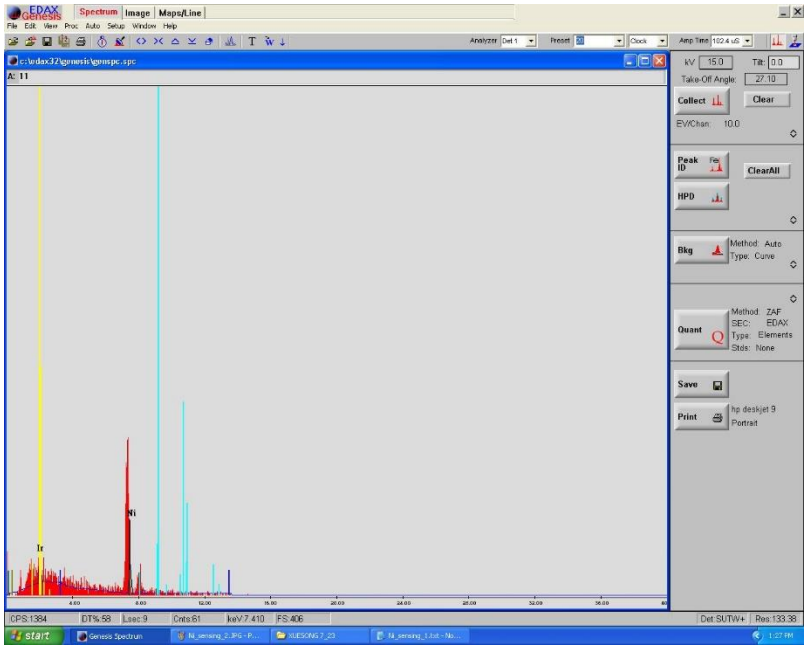

Figure 7: EDAX in the sensing area of the Ni-IROF based pH sensor

When the device was tested for sensitivity in different standard pH buffer solutions, it was shown that the sensor did not function outside the pH range of 4 to 10. As the range of pH that can be sensed by the device was limited, we needed to look for alternatives for the Ni-IROF

pH sensor. One way is to introduce an adhesion layer so that the metal electrode sticks firmly to the substrate. This allows us to use different adhesion layers.

4.1.2 Nickel thin film electrode with Cr adhesion layer

We took a 125 micron kapton and cleaned it according to standard cleaning procedure so that there are no dust particles on the substrate. Once it is confirmed that the substrate is good to be used, we spun a positive photoresist on the substrate to obtain uniform coating and then pre exposure bake was performed. We used a dark field mask and exposed it to UV light for specific time duration and developed it. The resultant pattern contains photoresist on the regions where we do not intend to deposit metal on the substrate. This means that, after lift-off we are left with metal deposited in the region where the electrode is expected.

We then deposited Cr followed by Ni using e-beam evaporation without releasing the chamber pressure. The deposition was done at a rate of 1-1.5 A/s. After the deposition, the substrate was placed in a bath containing acetone and was agitated gently so that the photoresist along with the metal on top of it is stripped away leaving the metal with the adhesion layer of Cr patterned in the desired way on the substrate. The samples were then cut from the substrate to ease the process of SU-8 coating and sol-gel treatment.

It was then required to cover the entire electrode barring the sensing area so that sol-gel treatment can be done. For this purpose, we needed a thick protective coat that could be peeled off after the process. We chose SU-8-100 which gives a pretty thick coating and can also be peeled very easily.

After this, the sol-gel dip coating process was accomplished and the SU-8 layer was peeled off.

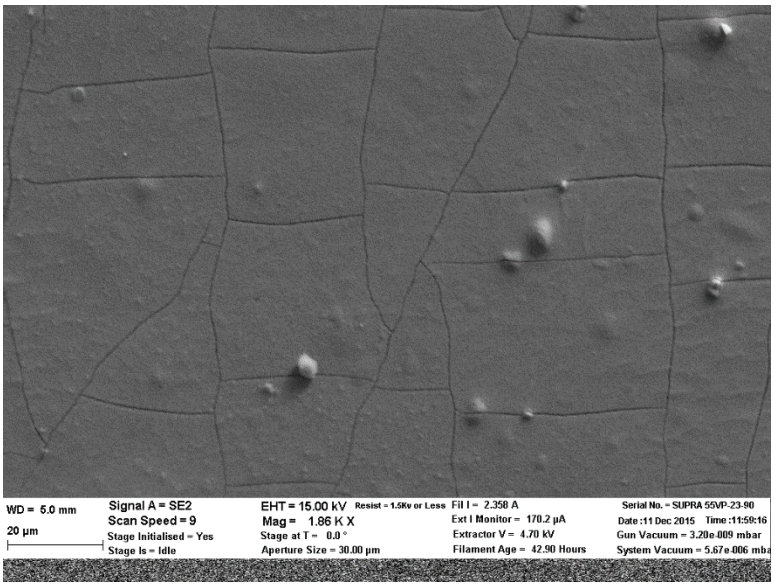

Figure 8: SEM of the sensing area of the Cr-Ni-IROF pH sensor

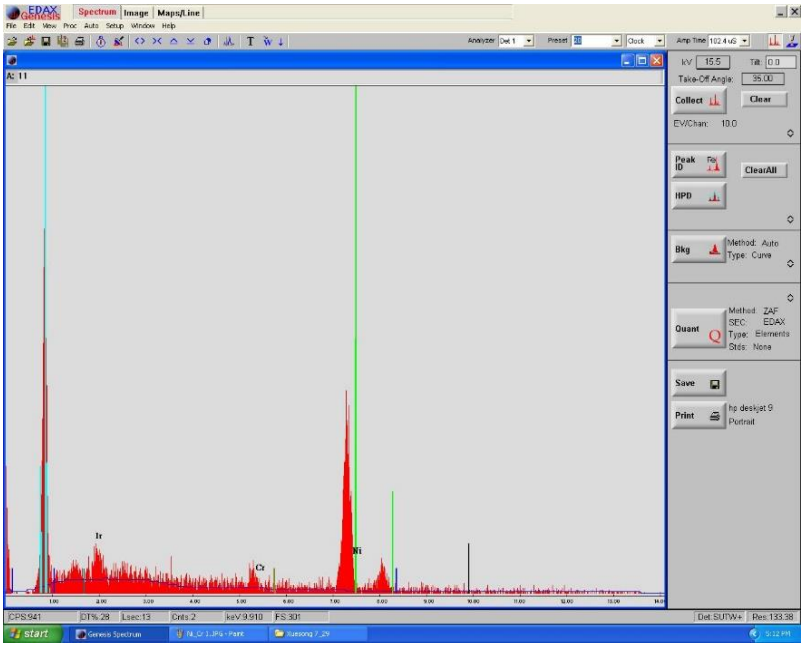

Figure 9: EDAX in the sensing area of the Cr-Ni-IROF based pH sensor

To form the IROF, the sequential thermal treatment, which was mentioned in the previous chapter, was performed. Then, SU-8-5 was used to create an insulation so that there is no

interference between the other parts of the metal electrode and the pH buffer solution during the sensitivity test. Figure 8 shows the SEM of the Cr-Ni-IROF based pH sensor. To understand the surface composition of the sensing area, we can make use of Energy Dispersive X-ray Spectroscopy (EDAX). The EDAX for the sensing area of the Cr-Ni-IROF pH sensor is presented in Figure 9.

4.1.3 Nickel thin film electrode with Ti adhesion layer

We took a 125 micron kapton and cleaned it according to standard cleaning procedure so that there are no dust particles on the substrate. Once it is confirmed that the substrate is good to be used, we spun a positive photoresist on the substrate to obtain uniform coating and then pre exposure bake was performed. We used a dark field mask and exposed it to UV light for specific time duration and developed it. The resultant pattern contains photoresist on the regions where we do not intend to deposit metal on the substrate. This means that, after lift-off we are left with metal deposited in the region where the electrode is expected.

We then deposited Ti followed by Ni using e-beam evaporation without releasing the chamber pressure. The deposition was done at a rate of 1-1.5 A/s. After the deposition, the substrate was placed in a bath containing acetone and was agitated gently so that the photoresist along with the metal on top of it is stripped away leaving the metal along with the adhesion layer of Ti patterned in the desired way on the substrate. The samples were then cut from the substrate to ease the process of SU-8 coating and sol-gel treatment.

It was then required to cover the entire electrode barring the sensing area so that sol-gel treatment can be done. For this purpose, we needed a thick protective coat that could be peeled

off after the process. We chose SU-8-100 which gives a pretty thick coating and can also be peeled very easily.

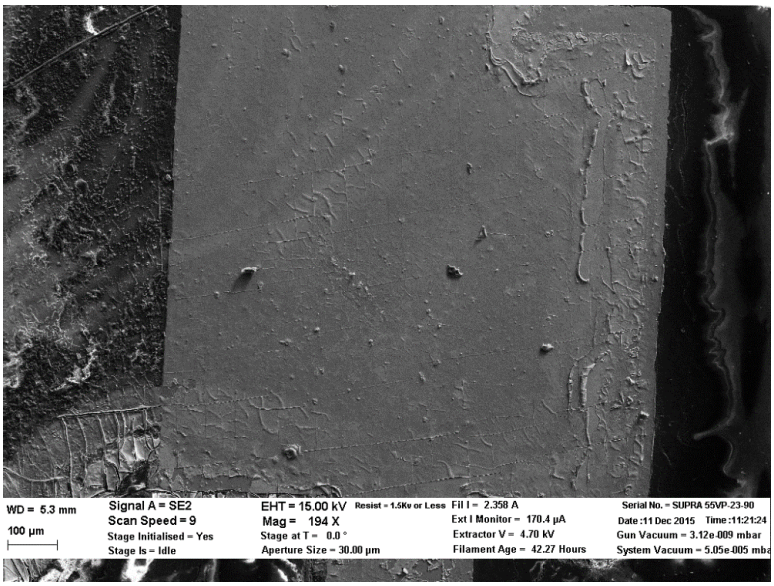

Figure 10: SEM of the sensing area of the Ti-Ni-IROF pH sensor

After this, the sol-gel dip coating process was accomplished and the SU-8 layer was peeled off. To form the IROF, the sequential thermal treatment, which was mentioned in the previous chapter, was performed. Then, SU-8-5 was used to create an insulation so that there is no interference between the other parts of the metal electrode and the pH buffer solution during the sensitivity test.

Figure 10 shows the SEM of the Ti-Ni-IROF based pH sensor. To understand the surface composition of the sensing area, we can make use of Energy Dispersive X-ray Spectroscopy (EDAX). The EDAX for the sensing area of the Ti-Ni-IROF pH sensor is presented in Figure 11.

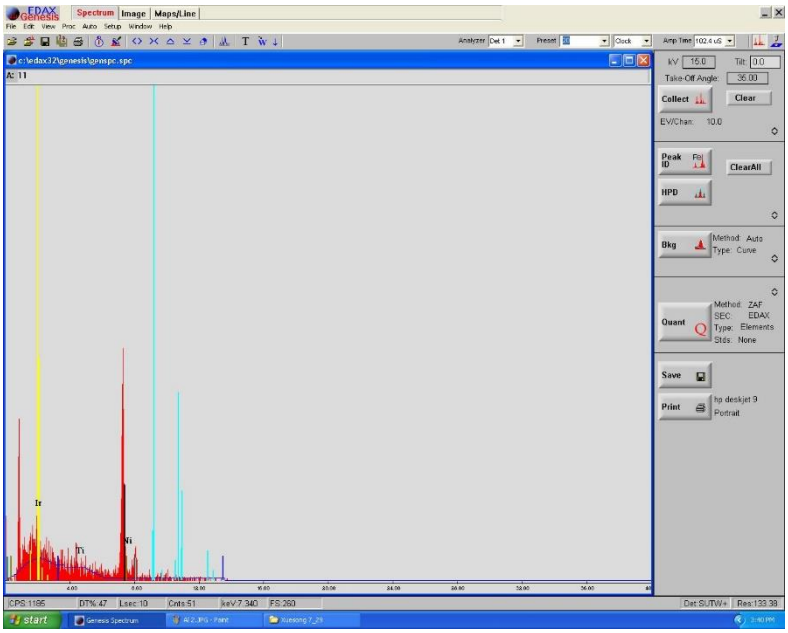

Figure 11: EDAX in the sensing area of the Ti-Ni-IROF based pH sensor

4.1.4 Nickel thin film electrode on a layer of sputtered carbon

We took a 125 micron kapton and cleaned it according to standard cleaning procedure so that there are no dust particles on the substrate. Once it is confirmed that the substrate is good to be used, we spun a positive photoresist on the substrate to obtain uniform coating and then pre exposure bake was performed. We used a dark field mask and exposed it to UV light for specific time duration and developed it. The resultant pattern contains photoresist on the regions where we do not intend to deposit metal on the substrate. This means that, after lift-off we are left with metal deposited in the region where the electrode is expected.

First we deposited carbon on the substrate using sputtering which was followed by deposition of Ni using e-beam evaporation. The deposition was done at a rate of 1-1.5 A/s. After the deposition, the substrate was placed in a bath containing acetone and was agitated gently so that the photoresist along with the metal on top of it is stripped away leaving the metal along

with the layer of carbon patterned in the desired way on the substrate. The samples were then cut from the substrate to ease the process of SU-8 coating and sol-gel treatment.

It was then required to cover the entire electrode barring the sensing area so that sol-gel treatment can be done. For this purpose, we needed a thick protective coat that could be peeled off after the process. We chose SU-8-100 which gives a pretty thick coating and can also be peeled very easily.

After this, the sol-gel dip coating process was accomplished and the SU-8 layer was peeled off. To form the IROF, the sequential thermal treatment, which was mentioned in the previous chapter, was performed. Then, SU-8-5 was used to create an insulation so that there is no interference between the other parts of the metal electrode and the pH buffer solution during the sensitivity test.

All these devices are tested and the results are presented in the next chapter. All the Ni based sensors were sensitive to the standard pH buffer solution in the range of 4-10. Using different adhesion layers gave better sensitivity in some cases and less potential fluctuations in other cases but did not make the sensor sensitive in the pH range below 4 and above 10. Hence, we made use of another metal to fabricate the electrodes, which is, Aluminum (Al).

4.2 Aluminum electrode based IROF pH sensor

4.2.1 Aluminum thin film electrode with no adhesion layer

The fabrication method used to fabricate Aluminum (Al) electrode is similar to that of Nickel. Al was deposited using both sputtering and electron beam evaporation but the sensitivity does not show any deviation from each other.

We took a 125 micron kapton and cleaned it according to standard cleaning procedure so that there are no dust particles on the substrate. Once it is confirmed that the substrate is good to be used, we spun a positive photoresist on the substrate to obtain uniform coating and then pre exposure bake was performed. We used a dark field mask and exposed it to UV light for specific time duration and developed it. The resultant pattern contains photoresist on the regions where we do not intend to deposit metal on the substrate. This means that, after lift-off we are left with metal deposited in the region where the electrode is expected.

We deposited Al using e-beam evaporation using Al pellets with a purity of 99.99%. The deposition was done at a rate of 1-1.5 A/s. After the deposition, the substrate was placed in a bath containing acetone and was agitated gently so that the photoresist along with the metal on top of it is stripped away leaving the metal electrode pattern in the desired way on the substrate. The samples were then cut from the substrate to ease the process of SU-8 coating and sol-gel treatment.

It was then required to cover the entire electrode barring the sensing area so that sol-gel treatment can be done. For this purpose, we needed a thick protective coat that could be peeled off after the process. We chose SU-8-100 which gives a pretty thick coating and can also be peeled very easily.

After this, the sol-gel dip coating process was accomplished and the SU-8 layer was peeled off. To form the IROF, the sequential thermal treatment, which was mentioned in the previous chapter, was performed. Then, SU-8-5 was used to create an insulation so that there is no interference between the other parts of the metal electrode and the pH buffer solution during the sensitivity test.

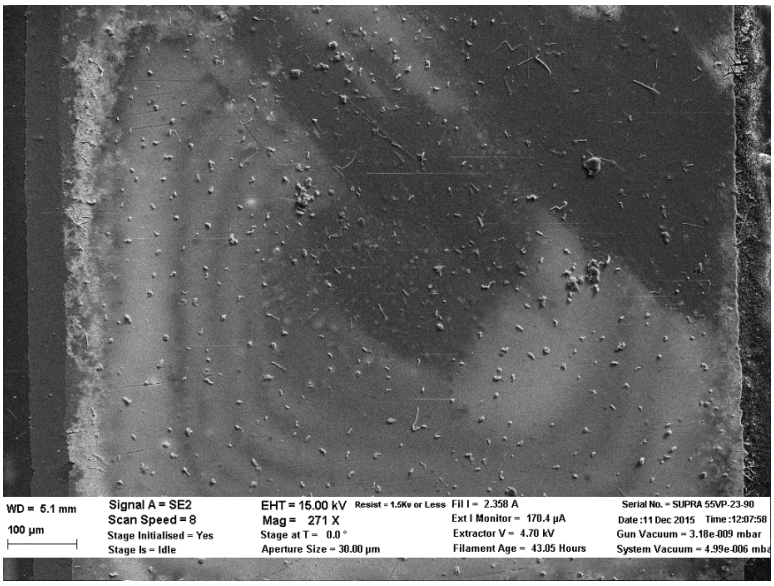

Figure 12: SEM of the sensing area of the Al-IROF pH sensor

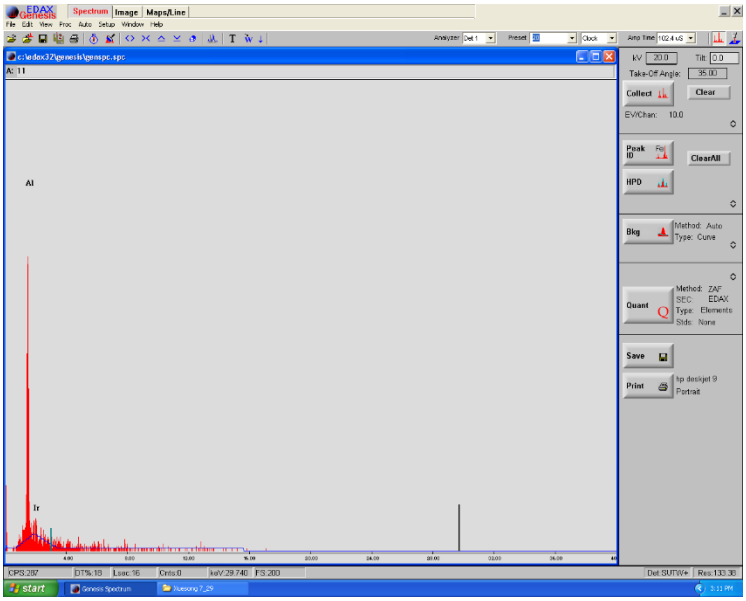

Figure 13: EDAX in the sensing area of the Al-IROF based pH sensor

Figure 12 shows the SEM of the Al-IROF based pH sensor. To understand the surface composition of the sensing area, we can make use of Energy Dispersive X-ray Spectroscopy (EDAX). The EDAX for the sensing area of the Al-IROF pH sensor is presented in Figure 13.

4.2.2 Aluminum thin film electrode with Ti adhesion layer

We took a 125 micron kapton and cleaned it according to standard cleaning procedure so that there are no dust particles on the substrate. Once it is confirmed that the substrate is good to be used, we spun a positive photoresist on the substrate to obtain uniform coating and then pre exposure bake was performed. We used a dark field mask and exposed it to UV light for specific time duration and developed it. The resultant pattern contains photoresist on the regions where we do not intend to deposit metal on the substrate. This means that, after lift-off we are left with metal deposited in the region where the electrode is expected.

We then deposited Ti followed by Al using e-beam evaporation without releasing the chamber pressure. The deposition was done at a rate of 1-1.5 A/s. After the deposition, the substrate was placed in a bath containing acetone and was agitated gently so that the photoresist along with the metal on top of it is stripped away leaving the metal along with the adhesion layer of Ti patterned in the desired way on the substrate. The samples were then cut from the substrate to ease the process of SU-8 coating and sol-gel treatment.

It was then required to cover the entire electrode barring the sensing area so that sol-gel treatment can be done. For this purpose, we needed a thick protective coat that could be peeled off after the process. We chose SU-8-100 which gives a pretty thick coating and can also be peeled very easily.

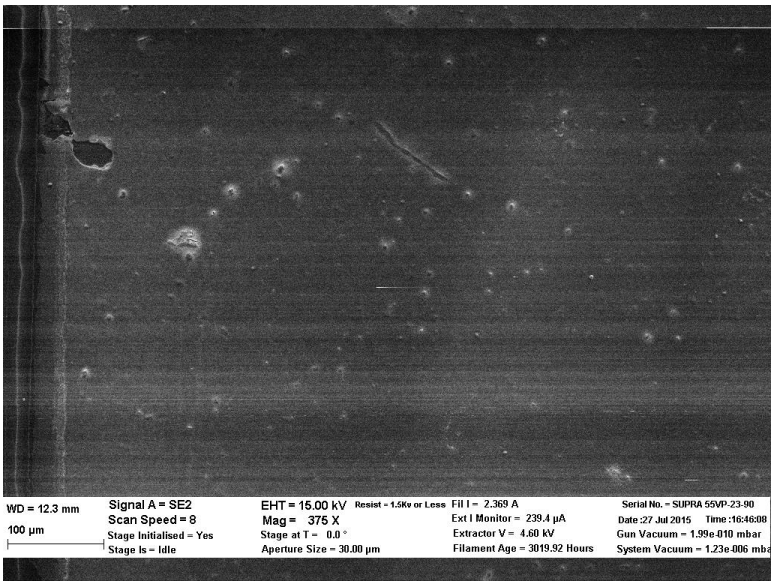

Figure 14: SEM of the sensing area of the Ti-Al-IROF pH sensor

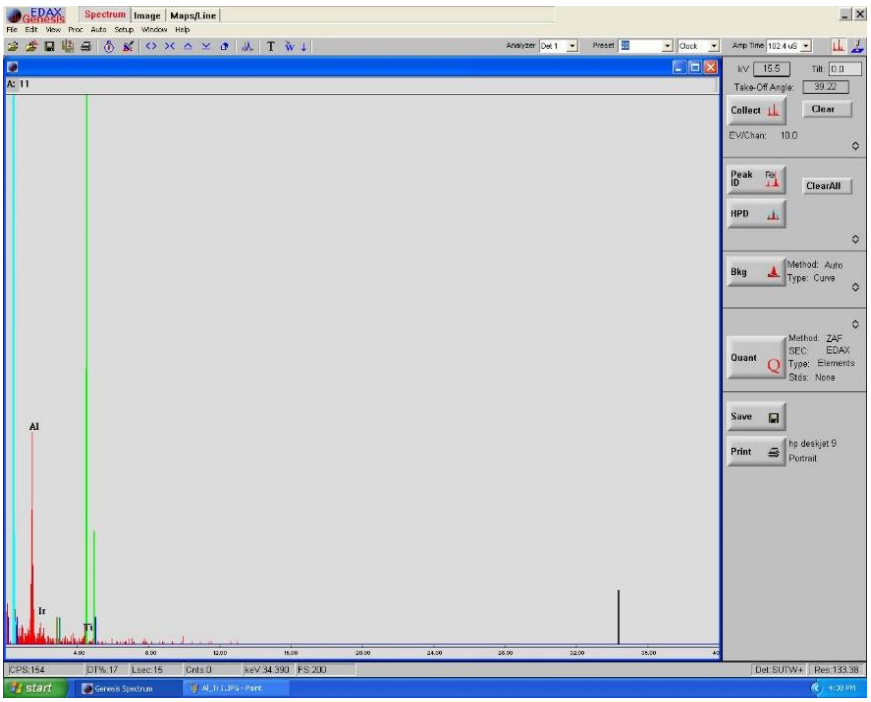

Figure 15: EDAX in the sensing area of the Ti-Al-IROF based pH sensor

After this, the sol-gel dip coating process was accomplished and the SU-8 layer was peeled off. To form the IROF, the sequential thermal treatment, which was mentioned in the previous chapter, was performed. Then, SU-8-5 was used to create an insulation so that there is no

interference between the other parts of the metal electrode and the pH buffer solution during the sensitivity test.

Figure 14 shows the SEM of the Ti-Al-IROF based pH sensor. To understand the surface composition of the sensing area, we can make use of Energy Dispersive X-ray Spectroscopy (EDAX). The EDAX for the sensing area of the Ti-Al-IROF pH sensor is presented in Figure 15.

4.3 Gold electrode based IROF pH sensor (Reference for comparison)

The similar can be said about the gold electrode fabrication using gold with a Cr adhesion layer. The next chapter discusses the testing methodology and the results obtained. The gold electrode upon sol-gel coating and thermal treatment followed by SU-8-5 insulation layer is shown in Figure 16 under an optical microscope. This gives a real time view of the sensing area.

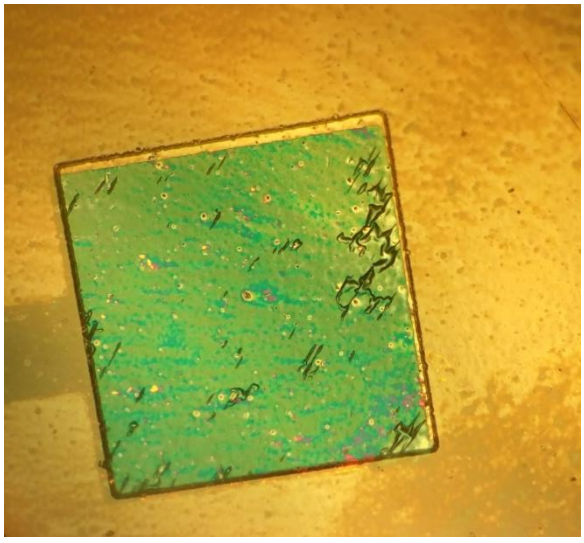

Figure 16: Optical microscope image of the sensing area of the Cr-Au-IROF pH sensor

CHAPTER FIVE: RESULTS

5.1 Testing Methodology

After the devices are fabricated with different metal electrodes, we need to test them to compare them for their performance. For this purpose, we use the metal electrode-IROF and an Ag/AgCl reference electrode. To test the performance, we use standard buffer solution with a foreknown pH value. The performance is analyzed using different performance parameters like sensitivity, repeatability and reversibility. Also, for each kind of metal electrode we can analyze the extrapolated potential value at pH=0. We know from theory that the values should be around 577mV. The test apparatus contains standard pH buffers like pH=2, pH=4, pH=7, pH=10 and pH=12. The metal-IROF electrode and the reference electrode are placed in the standard buffer solution and the potential between these two electrodes is measured using the National Instruments Data Acquisition (NI DAQ - 6009) tool. A lab view program is written so that a sample is taken every 0.1 seconds and the mean is taken for 10 samples obtained after each second.

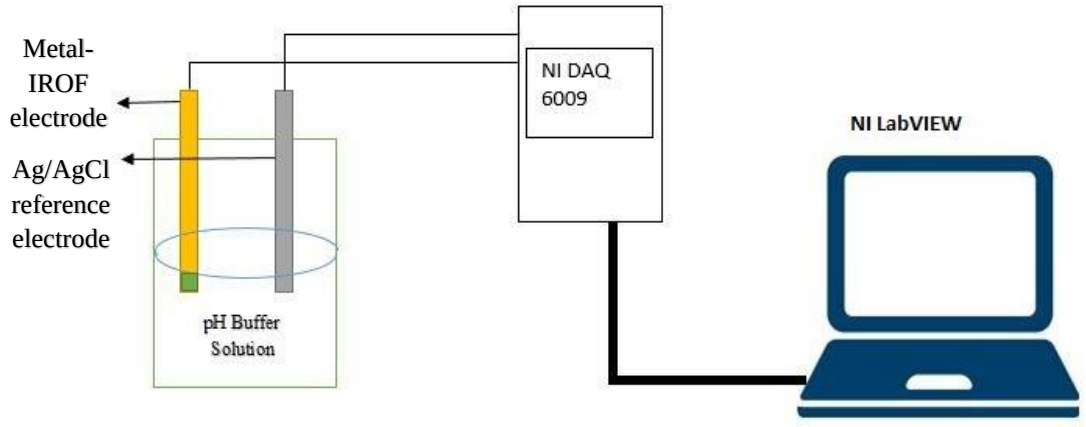

Figure 17: pH measurement set up

This average potential is plotted along with number of samples. The set is shown in figure 17. We used a commercial pH meter to measure the pH of the buffer solutions accurately. To judge the performance based on the quality of the IrO_x film we can take a look at the EDAX for the specific electrodes mentioned in the previous chapter. The various performance parameters are discussed in the following sections.

5.2 Sensitivity

The sensitivity of the sensors was tested and validated by using standard pH solutions with varying pH values starting from highly acidic buffer solution with pH=1.936 gradually increasing to a highly alkaline buffer solution with pH=11.698. The pH value of individual buffer solutions are measured using a commercial pH meter.

Initially our test sensor is that of a Ni-IROF. This sensor doesn't function as assumed in highly acidic as well as highly alkaline solutions. So, we test the sensor only in the range of pH values where it is sensitive. The same can be said for all Ni based pH sensors tested in this work. They are sensitive in the pH range starting from 3.94 to 9.623. The reason for this limitation is also discussed by providing an explanation using SEM to see the effect of highly acidic and alkaline solution on the Ni thin film. Then we introduce Al based pH sensors and their sensitivity. In Al based pH sensors this effect is eliminated and they function in the pH range of 1.936 to 11.698.

5.2.1 *Sensitivity of Ni-IROF based pH sensor*

As discussed above the Ni electrode IrO_x thin film based pH sensor only function in the pH range of 3.94 to 9.623. The sensor is tested in this range for 3 different pH values. The test was

repeated three times to look for consistency. We observe that the sensitivity is in the range of -57 mV/pH to -62 mV/pH with an average sensitivity of -59.12 mV/pH. Though the range is limited the sensitivity values are high when compared to the gold electrode based pH sensors presented in [41].

Also, they show a highly Nernstian response with an R^2 value of around 0.997 to 0.999. The test is repeated again with decreasing pH values starting from pH=9.623. The sensitivities are almost the same and the response is quick and consistent. The graphs in the below figures depict the sensitivities of the Ni electrode IrO_x thin film based pH sensor.

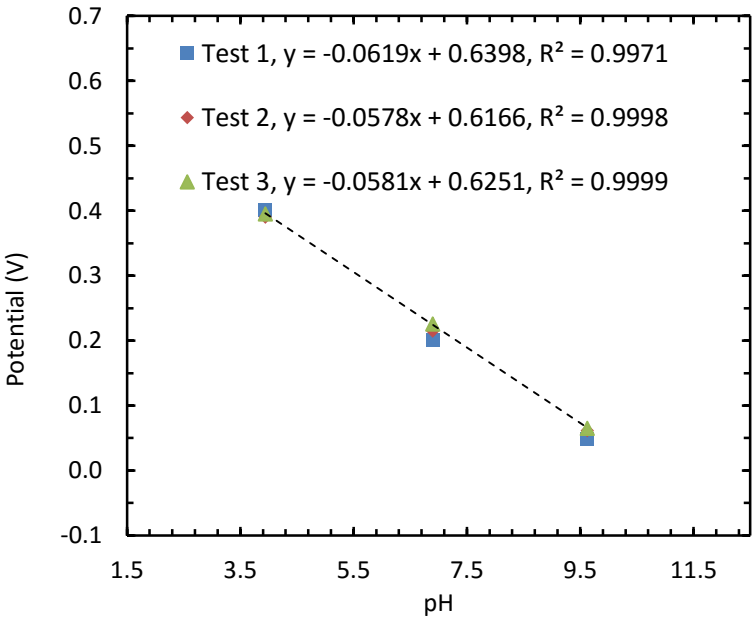

(a)

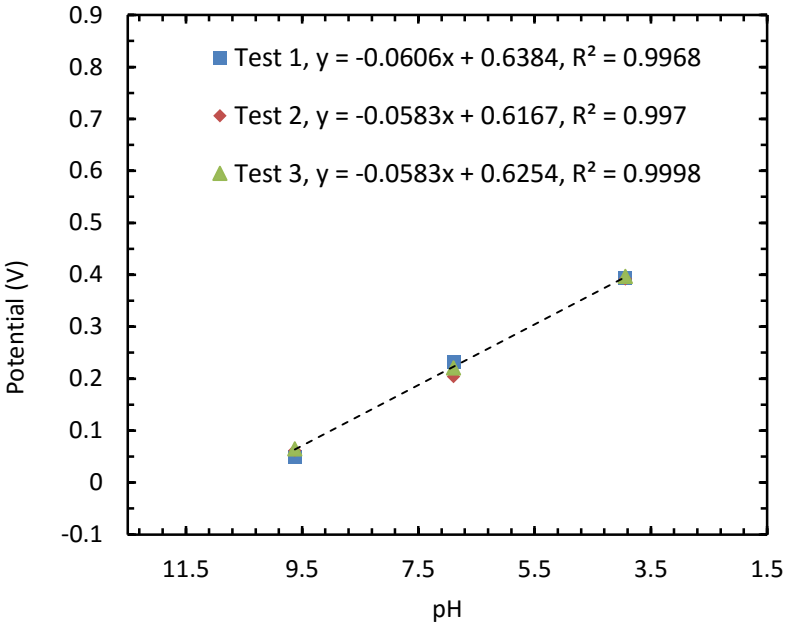

(b)

Figure 18: The Nernstian sensitivity responses Ni IrO_x thin film based pH sensor from (a) pH =3.94 to pH=9.623 (b) pH= 9.623 to pH= 3.94.

The potential in Volts shown on the y-axis of the figures above is the potential between the test electrode (the pH sensor) and the reference electrode (Ag/AgCl).

The sensors were also tested in highly acidic and highly alkaline pH solution which resulted in random response that was not consistent. Hence, to look at the surface so as to know what the effect was of highly acidic and highly alkaline solution on the thin films, we subjected the sensor to an SEM before and after contact with highly acidic and alkaline buffer solutions. The resultant SEM images showed that the surface of the sensing area got eroded or etched away. In other words they were affected by the highly acidic and alkaline solution. The SEM images are shown in the following figures.

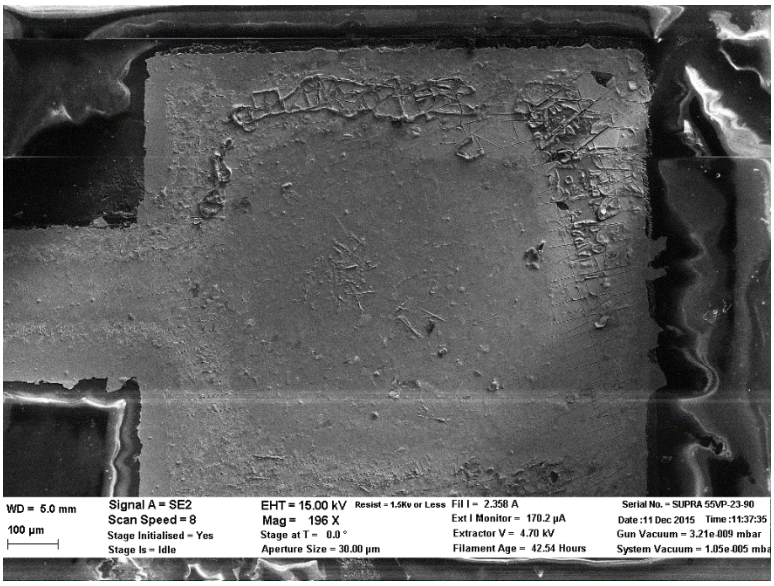

Figure 19: SEM of the sensing area of Ni-IROF pH sensor before testing.

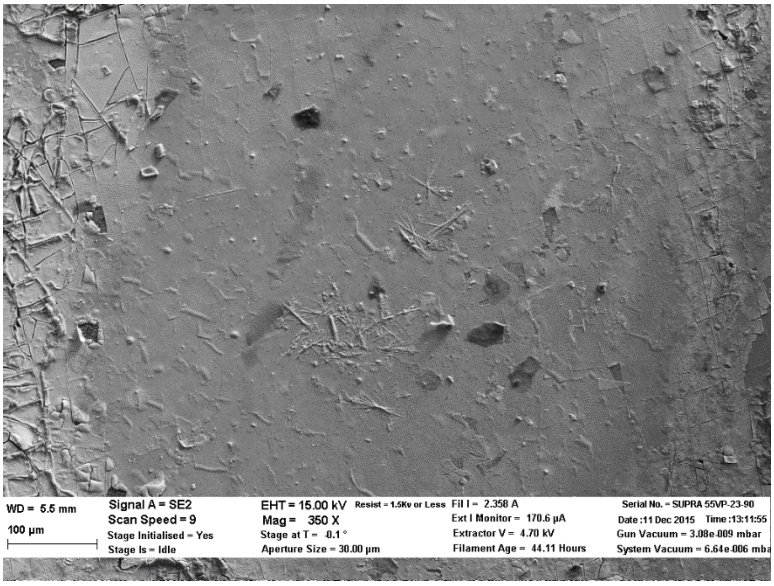

Figure 20: SEM of the sensing area of Ni-IROF pH sensor tested in pH ranging from 3.94 to 9.623.

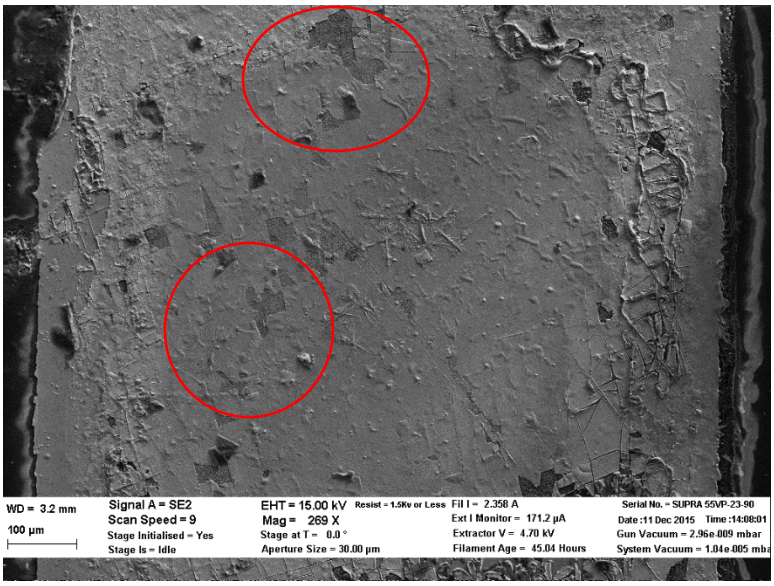

Figure 21: SEM of the sensing area of Ni-IROF pH sensor tested in pH of 1.936. The surface that was affected by the highly acidic buffer solution is also highlighted.

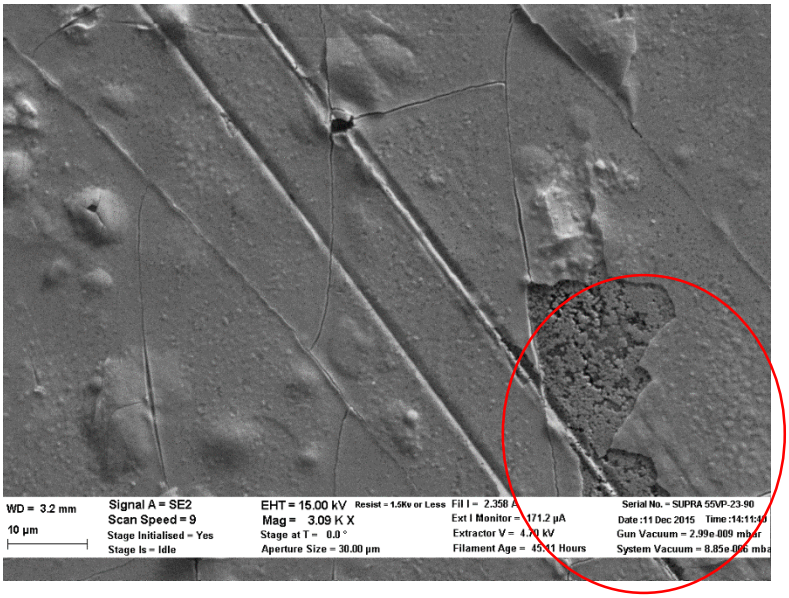

Figure 22: SEM of the sensing area of Ni-IROF pH sensor tested in pH of 11.698. The surface that was affected by the highly acidic buffer solution is also highlighted.

5.2.2 *Sensitivity of Cr-Ni-IROF based pH sensor*

To improve the performance and test the effect we introduced an adhesion layer to the above sensor. That is, we have fabricated the sensor using Ni with an adhesion layer of Cr and then introduced IrO_x thin film on the sensing area. The performance of this type of sensor is tested and compared with the other sensors in this text. The sensitivities were in the range of -54 mV/pH and -57 mV/pH when tested in the pH range of 3.94 to 9.623. The average sensitivity is around -55.9 mV/pH. We can see that the average sensitivity is slightly lower than the Ni-IROF based pH sensor. Also, they show a highly Nernstian response with an R^2 value of around 0.996 to 0.999. The test is repeated again with decreasing pH values starting from pH=9.623. The sensitivities are almost the same and the response is quick and consistent. The graphs in the below figures depict the sensitivities of the Cr-Ni electrode IrO_x thin film based pH sensor. The results are shown the following graphs.

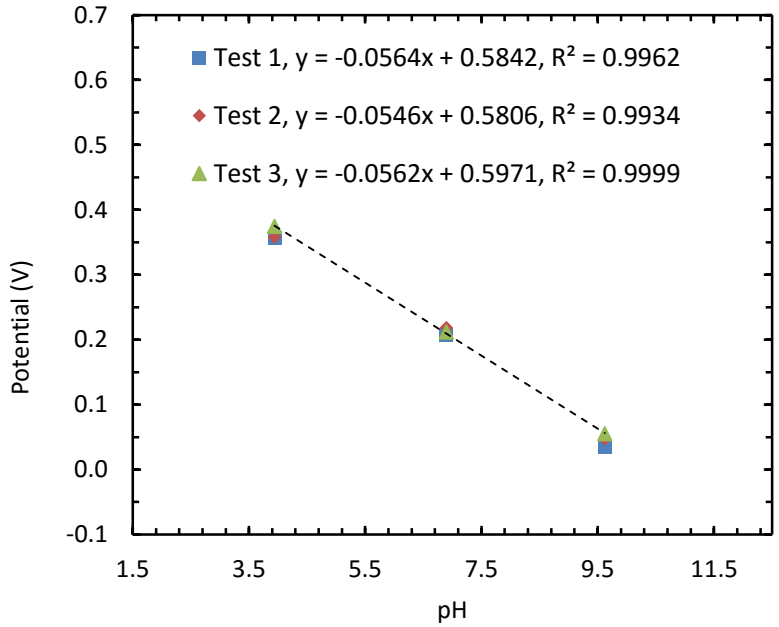

(a)

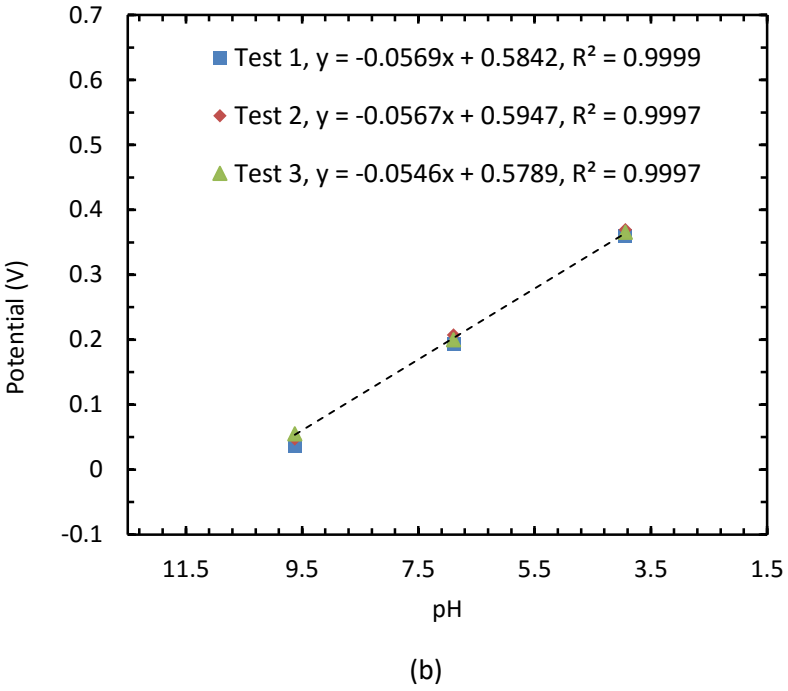

(b)

Figure 23: The Nernstian sensitivity responses Cr-Ni IrOx thin film based pH sensor from (a) pH =3.94 to pH=9.623 (b) pH= 9.623 to pH= 3.94.

The sensors were also tested in highly acidic and highly alkaline pH solution which resulted in random response that was not consistent. Hence, to look at the surface so as to know what the effect was of highly acidic and highly alkaline solution on the thin films, we subjected the sensor to an SEM before and after contact with highly acidic and alkaline buffer solutions.

The resultant SEM images showed that the surface of the sensing area got eroded or etched away. In other words they were affected by the highly acidic and alkaline solution. The SEM images are shown in the following figures.

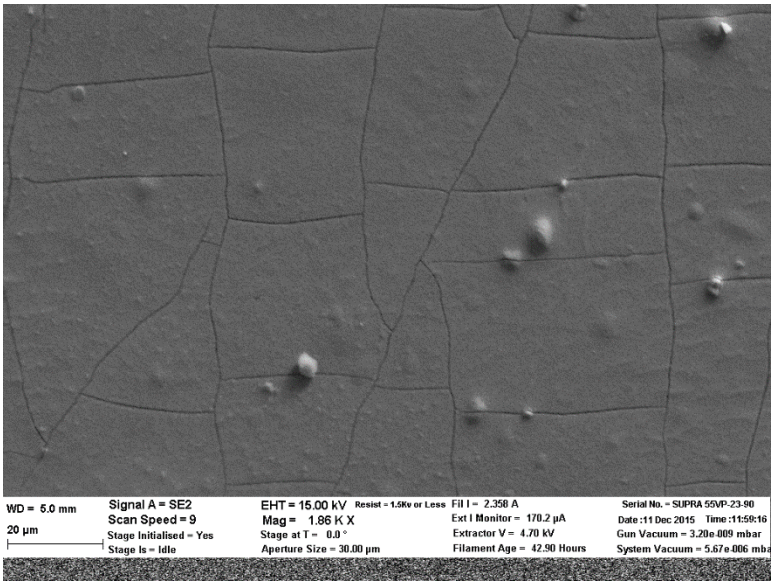

Figure 24: SEM of the sensing area of Cr-Ni-IROF pH sensor before testing

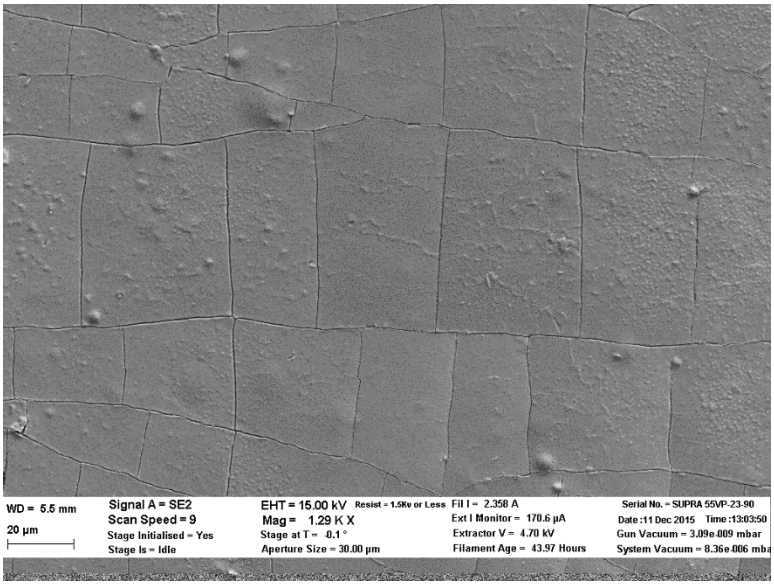

Figure 25: SEM of the sensing area of Cr-Ni-IROF pH sensor tested in pH ranging from 3.94 to 9.623.

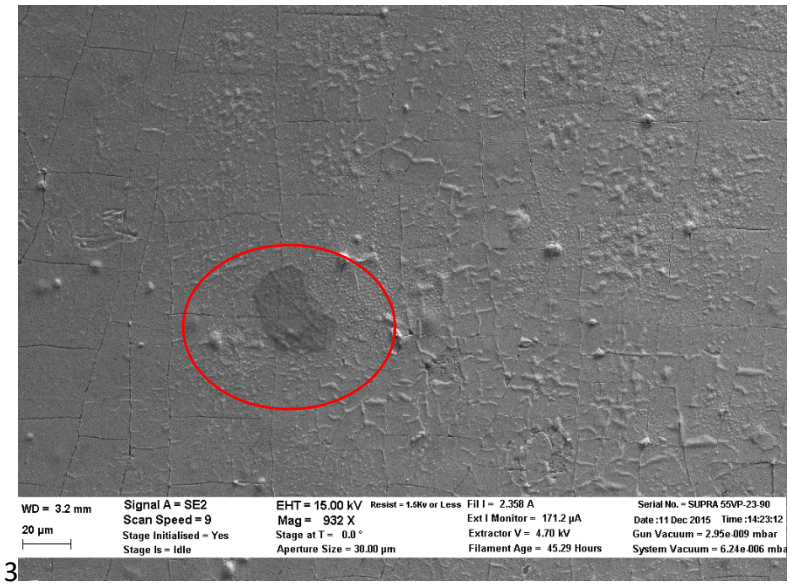

Figure 26: SEM of the sensing area of Cr-Ni-IROF pH sensor tested in pH of 1.936 and 11.698. The surface that was affected by the buffer solutions is also highlighted.

5.2.3 *Sensitivity of Ti-Ni-IROF based pH sensor*

We introduced another adhesion layer to the Ni-IROF based pH sensor. That is, we have fabricated the sensor using Ni with an adhesion layer of Ti and then introduced IrO_x thin film on the sensing area. The performance of this type of sensor is tested and compared with the other sensors in this text. The sensitivities were in the range of -54 mV/pH and -55 mV/pH when tested in the pH range of 3.94 to 9.623 with an exception of one test where the sensitivity dropped down to a value of -49mV/pH. The average sensitivity is around -53.6 mV/pH. We can see that the average sensitivity is slightly lower than the Ni-IROF and Cr-Ni-IROF based pH sensor. Also, they show a highly Nernstian response with an R^2 value of around 0.97 to 1. The test is repeated again with decreasing pH values starting from pH=9.623. The sensitivities are almost the same and the response is quick and consistent. The graphs in the below figures

depict the sensitivities of the Ti-Ni electrode IrO_x thin film based pH sensor. The results are shown in the following graphs.

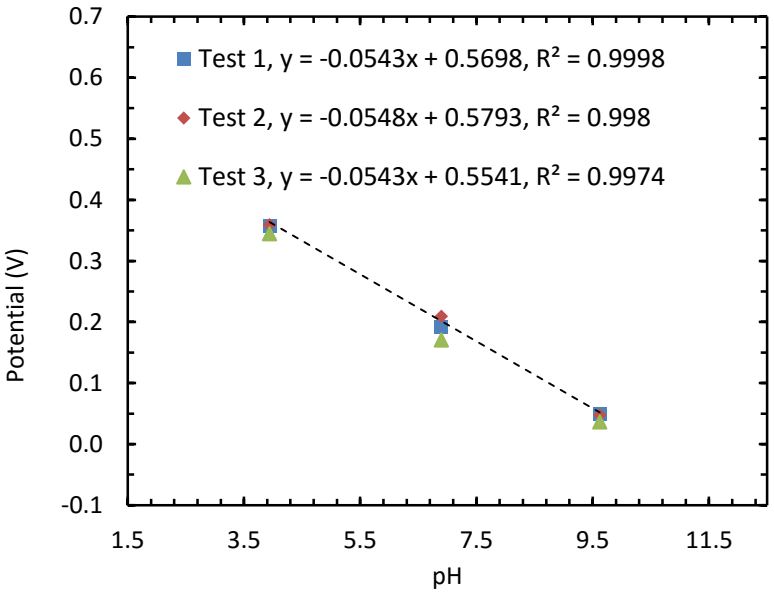

(a)

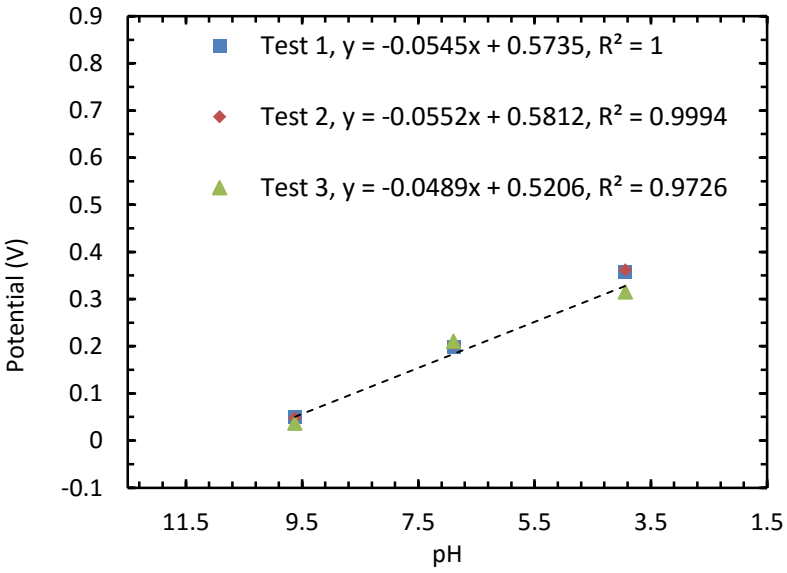

(b)

Figure 27: The Nernstian sensitivity responses Ti-Ni IrOx thin film based pH sensor from (a) pH =3.94 to pH=9.623 (b) pH= 9.623 to pH= 3.94.

The sensors were also tested in highly acidic and highly alkaline pH solution which resulted in random response that was not consistent. Hence, to look at the surface so as to know what the effect was of highly acidic and highly alkaline solution on the thin films, we subjected the sensor to an SEM before and after contact with highly acidic and alkaline buffer solutions.

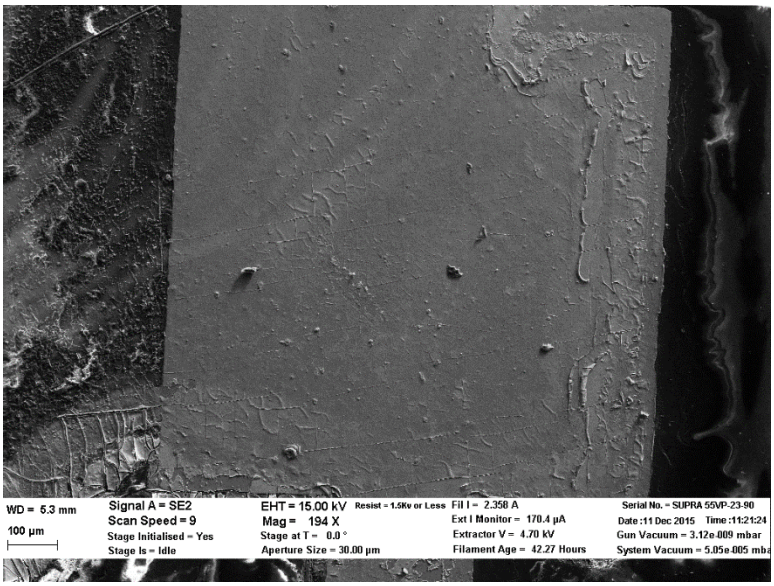

Figure 28: SEM of the sensing area of Ti-Ni-IROF pH sensor before testing

The resultant SEM images showed that the surface of the sensing area got eroded or etched away. In other words they were affected by the highly acidic and alkaline solution. The SEM images are shown in the figures 28-30.

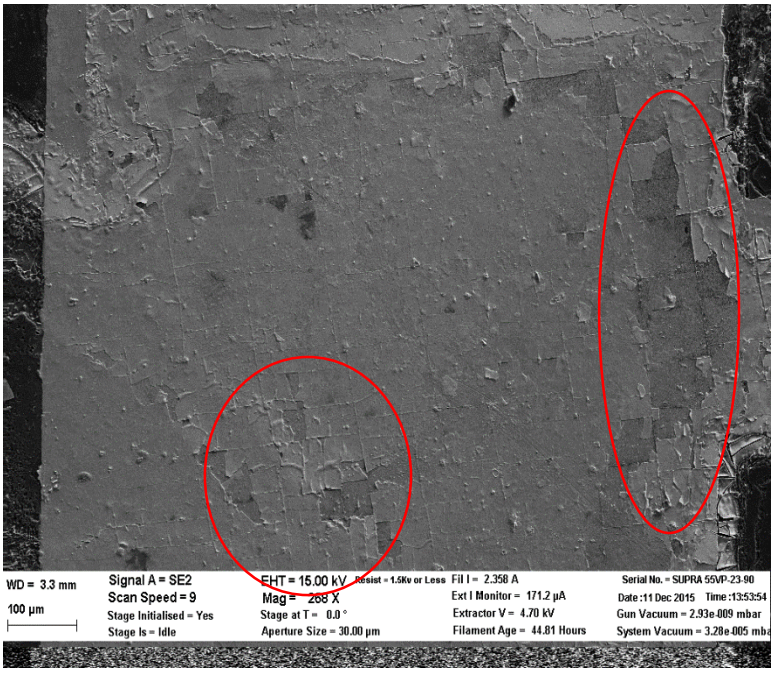

Figure 29: SEM of the sensing area of Ti-Ni-IROF pH sensor tested in pH of 1.936. The surface that was affected by the highly acidic buffer solution is also highlighted.

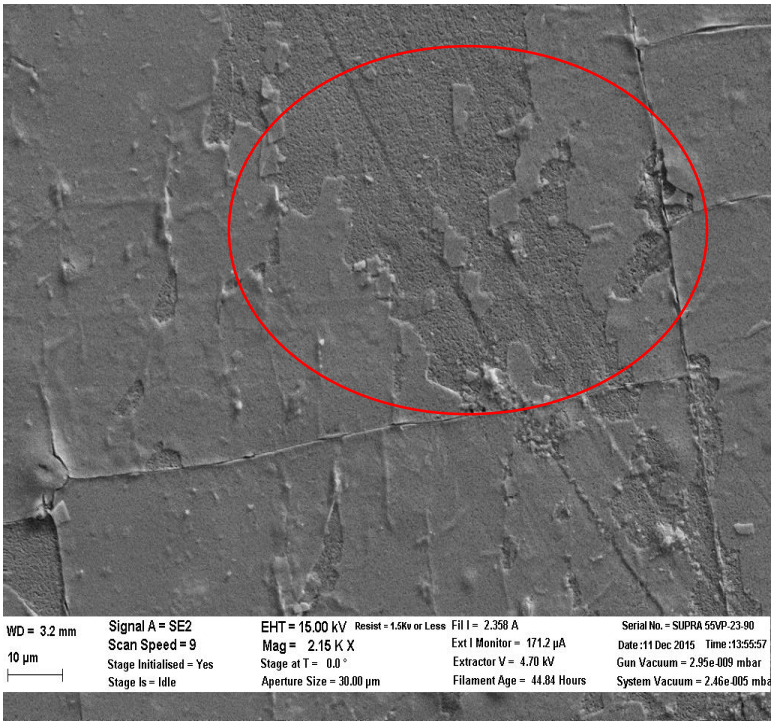

Figure 30: SEM of the sensing area of Ti-Ni-IROF pH sensor tested in pH of 11.698. The surface that was affected by the highly alkaline buffer solution is also highlighted.

5.2.4 *Sensitivity of C-Ni-IROF based pH sensor*

This time we introduced another layer to the Ni-IROF based pH sensor. That is, we have fabricated the sensor using Ni after introducing a layer of sputtered C and then introduced IrO_x thin film on the sensing area. The performance of this type of sensor is tested and compared with the other sensors in this text. The sensitivities were in the range of -43 mV/pH and -50 mV/pH when tested in the pH range of 3.94 to 9.623. The average sensitivity is around -46.05 mV/pH. We can see that the average sensitivity is way lower than the Ni-IROF, Cr-Ni-IROF, and Ti-Ni-IROF based pH sensor. But they show very high Nernstian response with an R^2 value of around 0.998 to 1. The test is repeated again with decreasing pH values starting from pH=9.623. The sensitivities are almost the same and the response is quick and consistent. The graphs in the below figures depict the sensitivities of the C-Ni electrode IrO_x thin film based pH sensor. The results are shown in the following graphs.

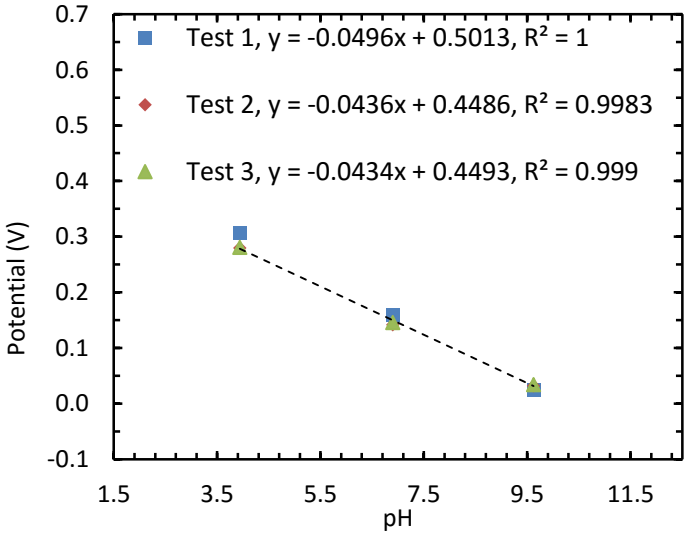

(a)

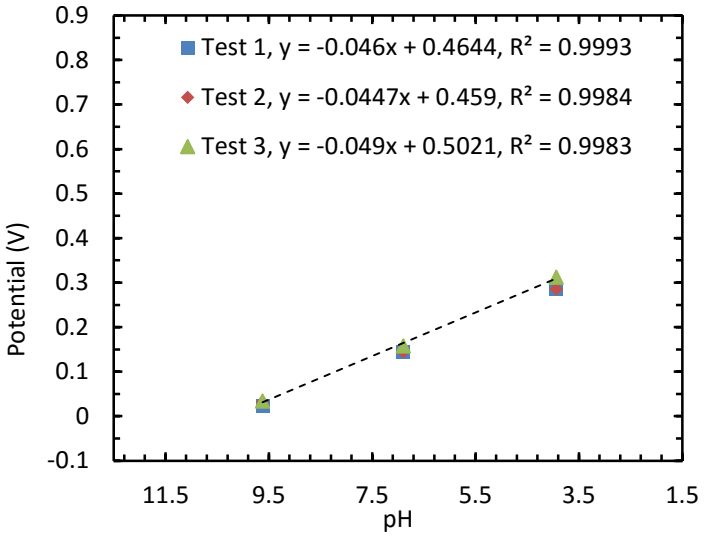

(b)

Figure 31: The Nernstian sensitivity responses C-Ni-IrOx thin film based pH sensor from (a) pH =3.94 to pH=9.623 (b) pH= 9.623 to pH= 3.94.

Though the sensitivities are lower, the advantage of using sputtered carbon before depositing Ni to form the electrode is that the fluctuation are very less when compared to other Ni based pH sensors.

A cumulative performance comparison is shown in figure 32. In this graph, sensitivities of all the Ni based sensor are shown for comparison sake. We can see that sensitivity of Ni-IROF sensor is superior compared to other Ni based pH sensors and also that C-Ni-IROF sensor has the least sensitivity value.

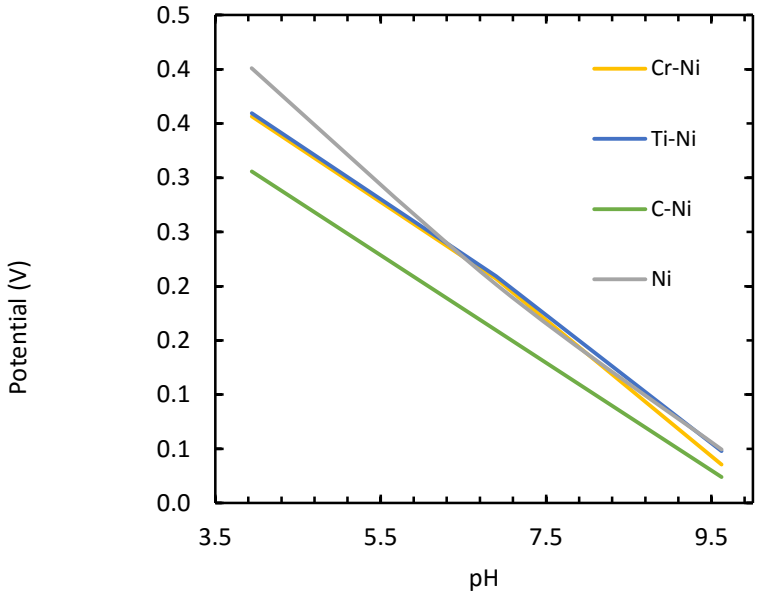

Figure 32: Sensitivity comparison of different Ni based sensors tested in the same pH range and in the same pH buffer solutions.

5.2.5 *Sensitivity of Al-IROF based pH sensor*

Now that we tested Ni based sensors and found the limitation that the sensors can only be used in a very narrow window of pH values, though they have high sensitivity, we need to look for alternatives which can be used for broad range of pH values. We, therefore, use Aluminum as an alternative and the results are as follows.

As discussed in the previous chapter Al electrode IrO_x thin film based pH sensor function in a broad pH range and are tested in the pH range of 1.936 to 11.698. The sensor is tested in this range for 5 different pH values. The test was repeated three times to look for consistency. We observe that the sensitivity is in the range of -48 mV/pH to -55 mV/pH with an average sensitivity of -50.87 mV/pH. Also, they show a highly Nernstian response with an R^2 value of

around 0.988 to 0.995. The test is repeated again with decreasing pH values starting from pH=11.698. The sensitivities are almost the same and the response is quick and consistent. The graphs in the below figures depict the sensitivities of the Al electrode IrO_x thin film based pH sensor.

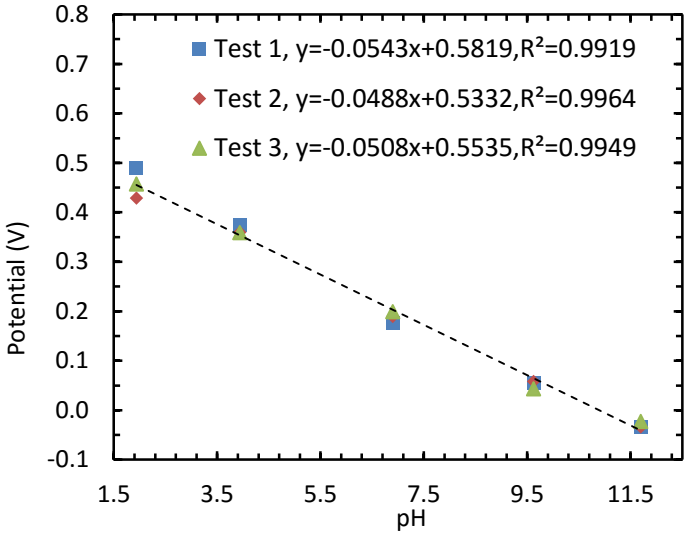

(a)

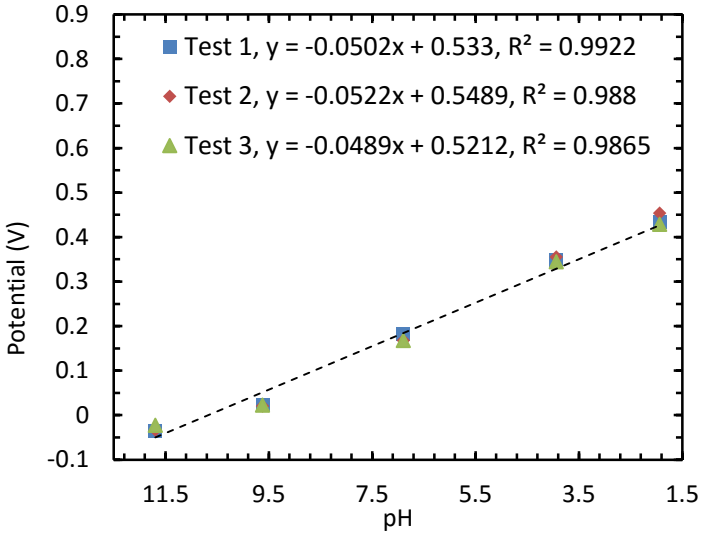

(b)

Figure 33: The Nernstian sensitivity responses Al-IrOx thin film based pH sensor from (a) pH =1.936 to pH=11.698 (b) pH= 11.698 to pH= 1.936.

We saw that the Al-IROF based pH sensor works in the broad pH range which includes highly acidic as well as highly alkaline pH ranges. We looked at the surface closely before and after contact with these extreme pH levels under SEM and saw that there is no effect on the surface of Al-IROF pH sensor and hence we can confirm that the Ni based sensors did not give good pH sensitivity in these extreme pH ranges due to the fact that the surface got altered or affected.

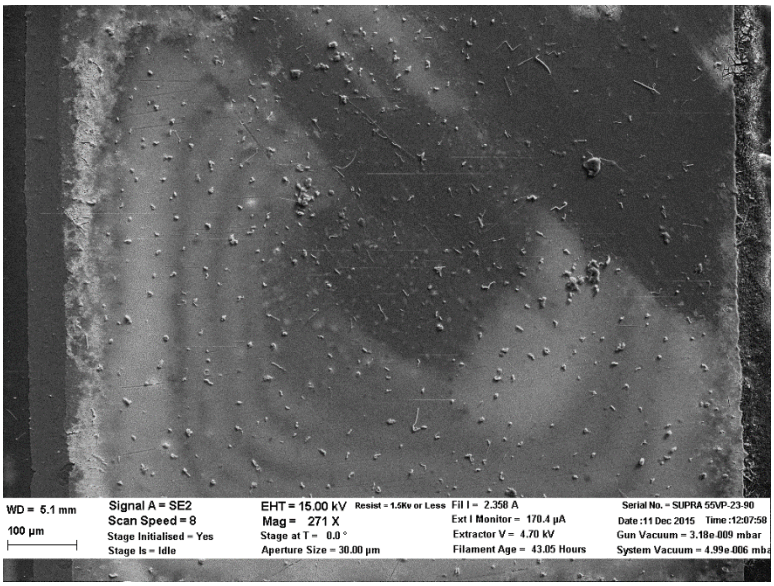

Figure 34: SEM of the sensing area of Al-IROF pH sensor before testing

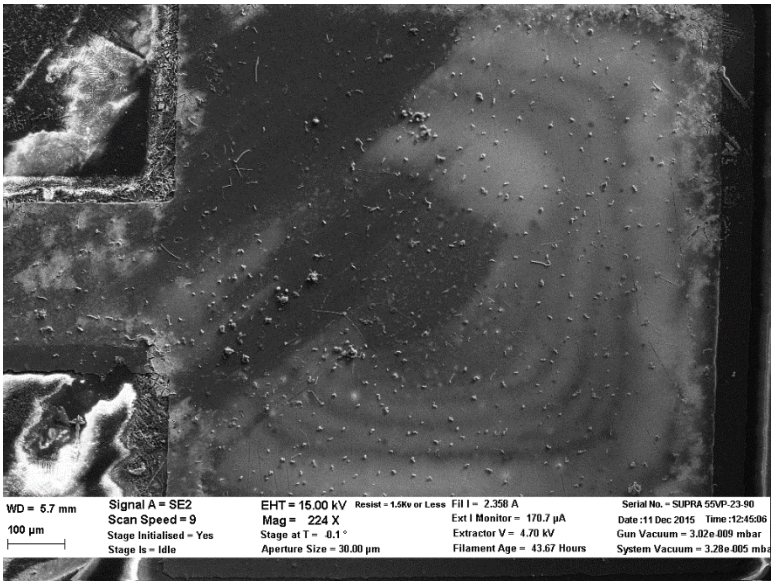

Figure 35: SEM of the sensing area of Ti-Ni-IROF pH sensor tested in pH range of 1.936 to 11.698.

5.2.6 *Sensitivity of Ti-Al-IROF based pH sensor*

With an aim to enhance the performance of the Al-IROF based pH sensor, we introduced an adhesion layer to the Al-IROF based pH sensor. That is, we have fabricated the sensor using Al with an adhesion layer of Ti and then introduced IrOx thin film on the sensing area. The performance of this type of sensor is tested and compared with the other sensors in this text. The sensitivities were in the range of -59 mV/pH and -61 mV/pH when tested in the pH range of 1.936 to 11.698. The average sensitivity is around -60.03 mV/pH. We can see that the average sensitivity is higher than all other pH sensors discussed above. Also, this type of pH sensor showed a highly Nernstian response with an R2 value of around 0.998 to 0.9996. The test is repeated again with decreasing pH values starting from pH=11.698. The sensitivities are almost the same and the response is quick and consistent. The graphs in the below figures depict the sensitivities of the Ti-Al electrode IrOx thin film based pH sensor. The results are shown in the following graph.

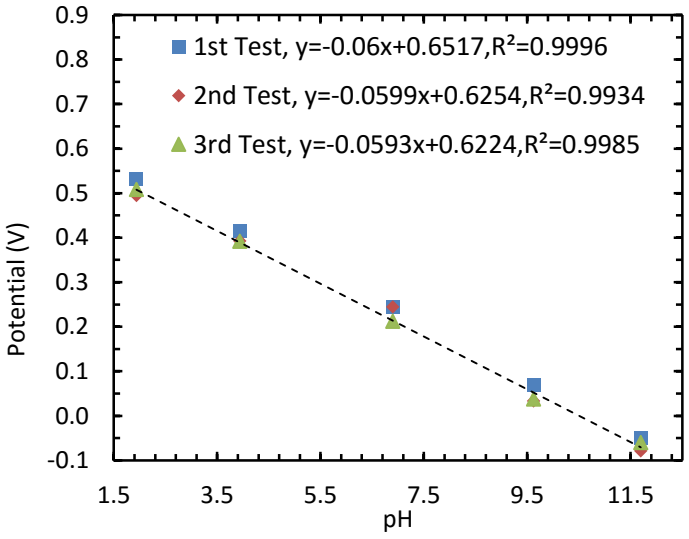

(a)

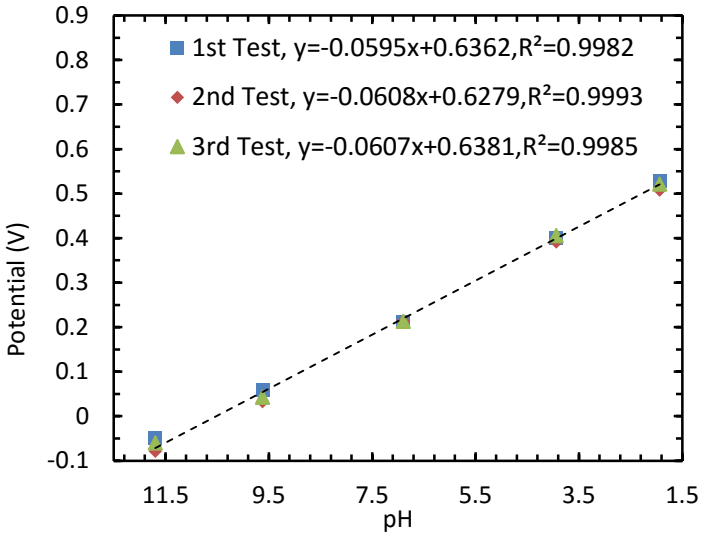

(b)

Figure 36: The Nernstian sensitivity responses Ti-Al-IrOx thin film based pH sensor from (a) pH =1.936 to pH=11.698 (b) pH= 11.698 to pH= 1.936.

A cumulative performance comparison is shown in figure 37. In this graph, sensitivities of all the Al based sensor are shown for comparison sake. We can see that sensitivity of Ti-Al-IROF sensor is superior compared to Al-IROF pH sensor.

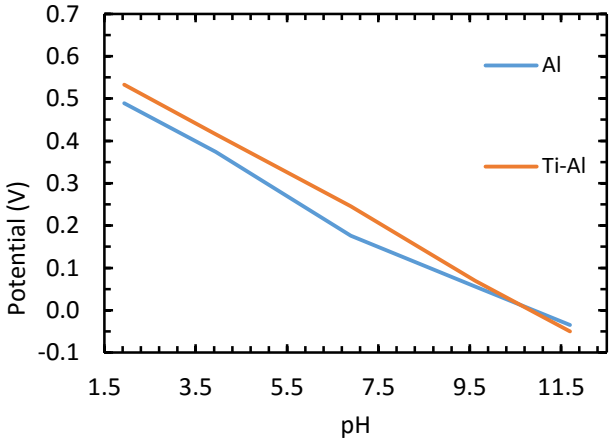

Figure 37: Sensitivity comparison of different Al based sensors tested in the same pH range and in the same pH buffer solutions.

5.2.7 *Sensitivity of Cr-Au-IROF based pH sensor*

Now, we fabricate the sensor to which all the above sensor are to be compared in terms of performance parameter. That is the Gold-IROF pH sensor. The performance of this type of sensor is tested and compared with the other sensors in this text. The sensitivities were in the range of -44 mV/pH and -47 mV/pH when tested in the pH range of 1.936 to 11.698. The average sensitivity was 45.15 mV/pH. Also, they show a highly Nernstian response with an R^2 value of around 0.995 to 0.997. The test is repeated again with decreasing pH values starting from pH=11.698. The sensitivities are almost the same and the response is quick and consistent. The graphs in the below figures depict the sensitivities of the Au electrode IrO_x thin film based pH sensor.

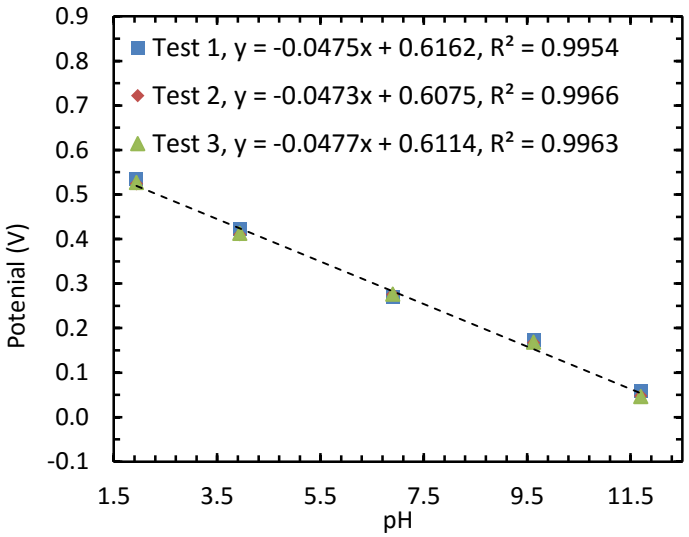

(a)

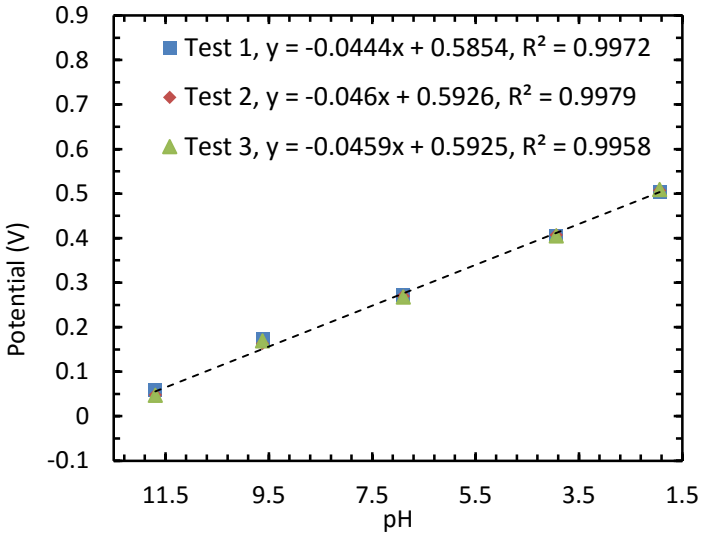

(b)

Figure 38: The Nernstian sensitivity responses Cr-Au-IrOx thin film based pH sensor from (a) pH =1.936 to pH=11.698 (b) pH= 11.698 to pH= 1.936.

Figure 39 shows a comparison of all the sensors tested in this research work.

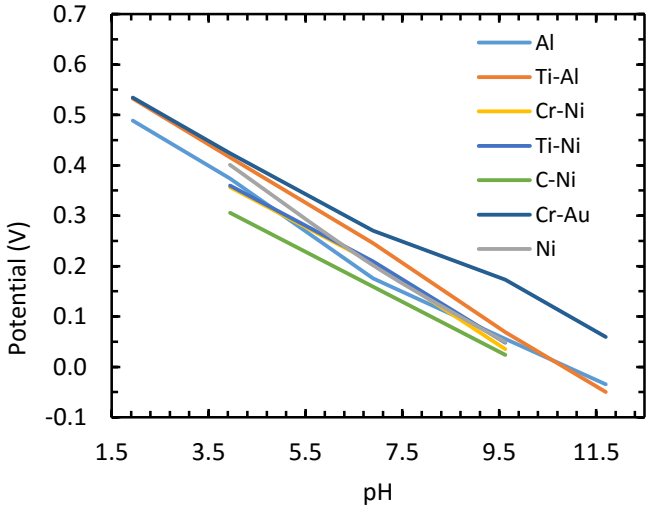

Figure 39: Sensitivity comparison of different Ni, Al and Au based sensors tested in the same pH range and in the same pH buffer solutions.

We have seen in this section about the sensitivities of each type of sensor and compared the sensitivity values. We know that for reference Ag/AgCl electrode the potential obtained when the graph is extrapolated to pH=0 must be close to 577 mV. We have tabulated this potential obtained from extrapolation of the sensitivity graphs. In total we have 6 tests for each sensor hence we have taken the average of this value obtained from each graph and obtained the average potential value which has been tabulated.

TYPE OF SENSOR	Potential at pH=0 (mV)
Ni-IROF	627
Cr-Ni-IROF	586.6
Ti-Ni-IROF	563.1
C-Ni-IROF	470.8
Al-IROF	545.3
Ti-Al-IROF	633.6
Cr-Au-IROF	600.1

Table 1: Potential between metal-IROF electrode and Ag/AgCl reference electrode at pH=0 found by extrapolation

5.3 Reversibility and Repeatability

Though it is vague to discuss reversibility and repeatability of sensors, we use the parameters mentioned in [41] to understand the reversibility and repeatability. For this, we have used parameters mentioned in the literature, which are, potential fluctuation (ΔV), potential deviation (δV), and potential drift (V'). In addition to these parameters there is also another parameter called the hysteresis (dV). We have used the reference diagram that has been mentioned in [41] to understand all the parameters.

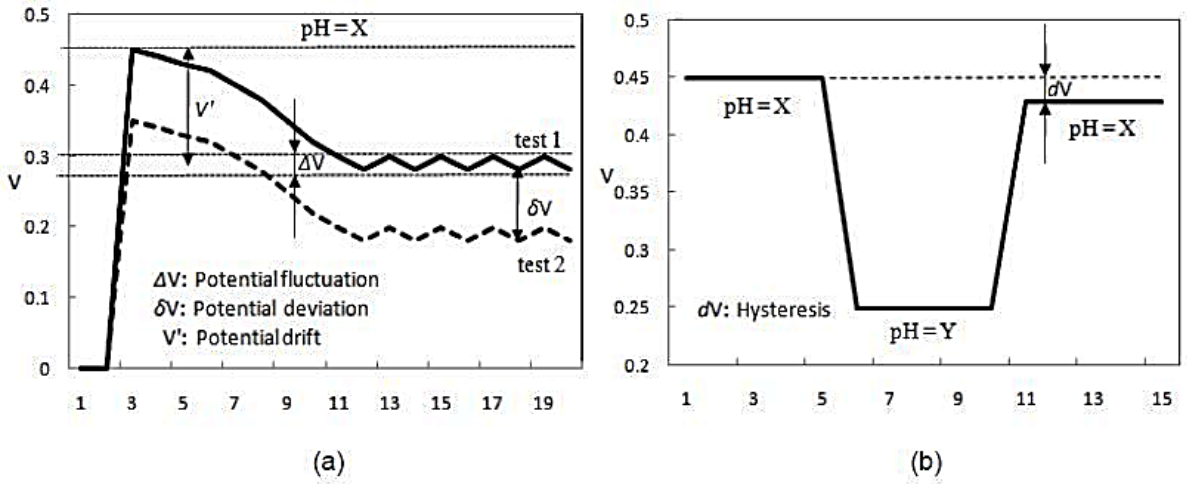

Figure 40: Pictorial depiction of (a) Potential drift, fluctuation and deviation (b) hysteresis

ΔV is the stable, small, and non-random voltage fluctuating range which occurs after the electrochemical potential reaches a stable value. The potential fluctuation may be caused due to many reasons including the noise from the recording instrument or unstable source interference such as stirring or liquid movement during the test. δV is the potential difference between the different tests of the same electrode in the same buffer solutions. The potential deviation may be caused due to the oxidation state and the surface OH^- ion exchange of iridium oxide. This may shift the equilibrium slightly which causes surface charge [21, 44-45]. Potential drift V' is defined as the potential shift which is from the peak potential value to 90% of the equilibrium potential value as showed in figure 40. The potential drift may be caused by some reasons such as the procedure of temperature affection, sensor age, and different fabrication methods [21].

The sensor is tested three times in the same pH solutions in the pH range for which the device is functioning. The test is different from sensitivity test in the way that for the test of sensitivity the sensor is placed in a pH buffer solution and the potential between the sensing electrode and

the Ag/AgCl electrode is noted. Then, in the next step, before placing the sensor in the next standard pH solution we clean it with de-ionized (DI) water and blow it dry using a jet of dry N_2. But in this test, the sensors are continuously tested in one pH after another without cleaning the surface and data is continuously monitored. All the data is then plotted with potential between sensing electrode and Ag/AgCl reference electrode on y-axis and the sample number on x-axis. Repeating the test three times also lets us now the repeatability of the device.

5.3.1 *Reversibility and repeatability test on Ni-IROF based pH sensor*

The sensor was able to detect 5 different pH solutions from 3.94 to 9.623 and showed reversibility when tested in the decreasing order of pH. The graph in the following figure shows the test for reversibility and repeatability.

We can see from the figure that the sensors are fairly reversible and repeatable.

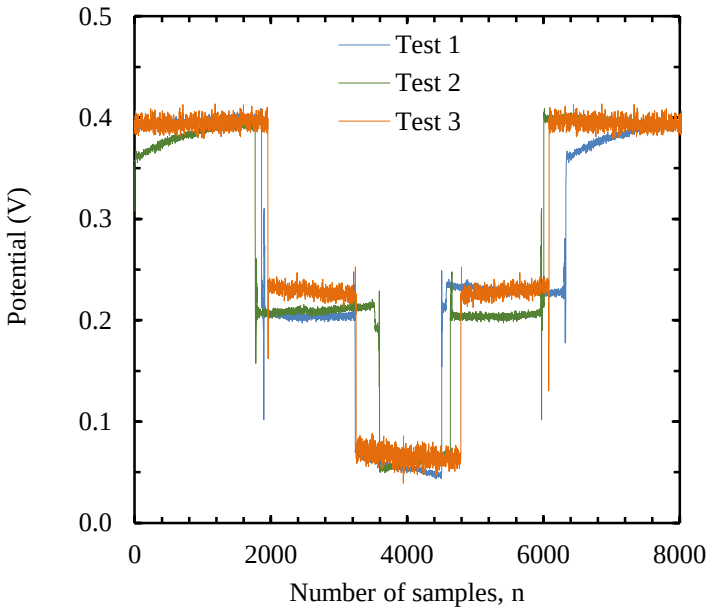

Figure 41: Reversibility and repeatability test performed on Ni-IROF pH sensor with the pH testing sequence 3.94 – 9.623 – 3.94

5.3.2 *Reversibility and repeatability test on Cr-Ni-IROF based pH sensor*

The sensor was able to detect 5 different pH solutions from 3.94 to 9.623 and showed reversibility when tested in the decreasing order of pH. The graph in the following figure shows the test for reversibility and repeatability.

We can see from the figure that the sensors are fairly reversible and repeatable.

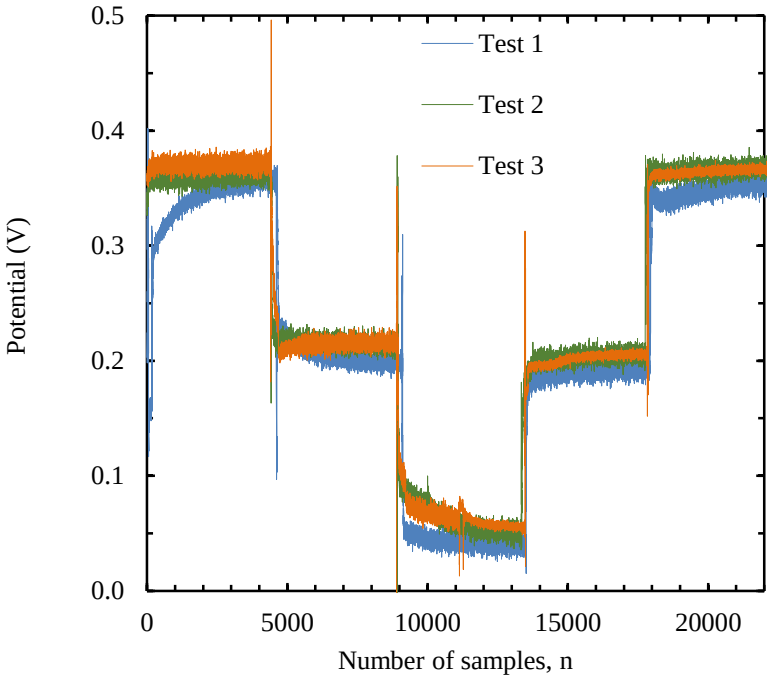

Figure 42: Reversibility and repeatability test performed on Cr-Ni-IROF pH sensor with the pH testing sequence 3.94 – 9.623 – 3.94

5.3.3 *Reversibility and repeatability test on Ti-Ni-IROF based pH sensor*

The sensor was able to detect 5 different pH solutions from 3.94 to 9.623 and showed reversibility when tested in the decreasing order of pH. The graph in the following figure shows the test for reversibility and repeatability.

We can see from the figure that the sensors are fairly reversible and repeatable.

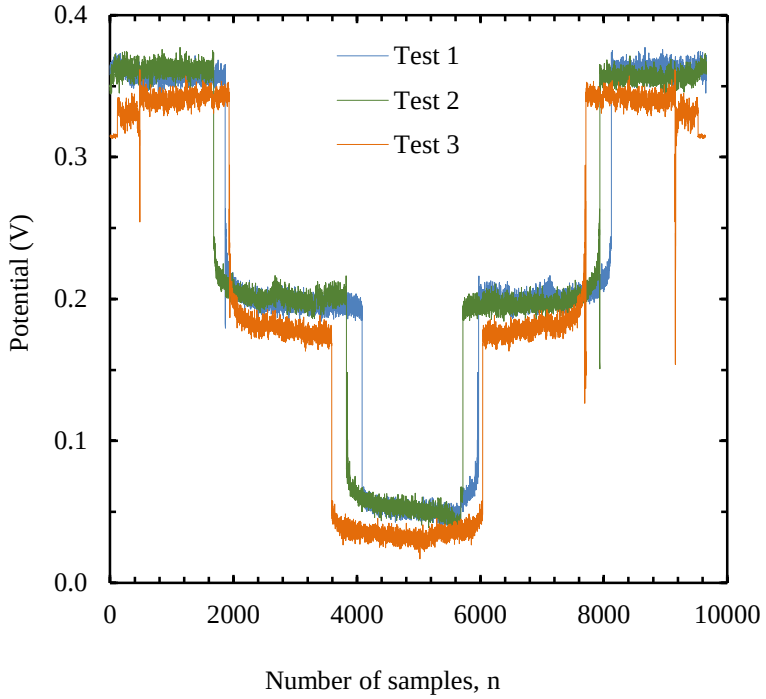

Figure 43: Reversibility and repeatability test performed on Ti-Ni-IROF pH sensor with the pH testing sequence 3.94 – 9.623 – 3.94

5.3.4 *Reversibility and repeatability test on C-Ni-IROF based pH sensor*

The sensor was able to detect 5 different pH solutions from 3.94 to 9.623 and showed reversibility when tested in the decreasing order of pH. The graph in the following figure shows the test for reversibility and repeatability.

We can see from the figure that the sensors are fairly reversible and repeatable.

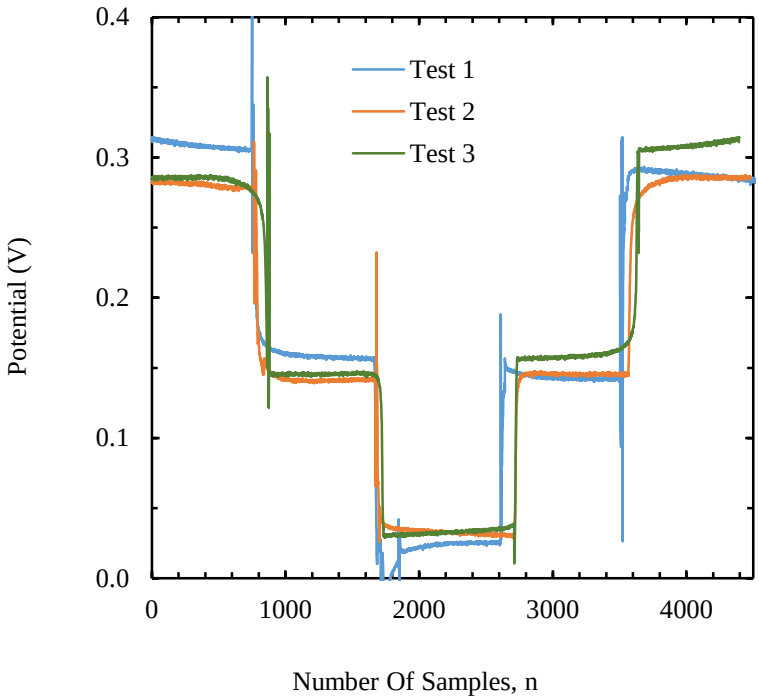

Figure 44: Reversibility and repeatability test performed on C-Ni-IROF pH sensor with the pH testing sequence 3.94 – 9.623 – 3.94

5.3.5 *Reversibility and repeatability test on Al-IROF based pH sensor*

The sensor was able to detect 5 different pH solutions from 1.936 to 11.698 and showed reversibility when tested in the decreasing order of pH. The graph in the following figure shows the test for reversibility and repeatability.

We can see from the figure that the sensors are fairly reversible and repeatable.

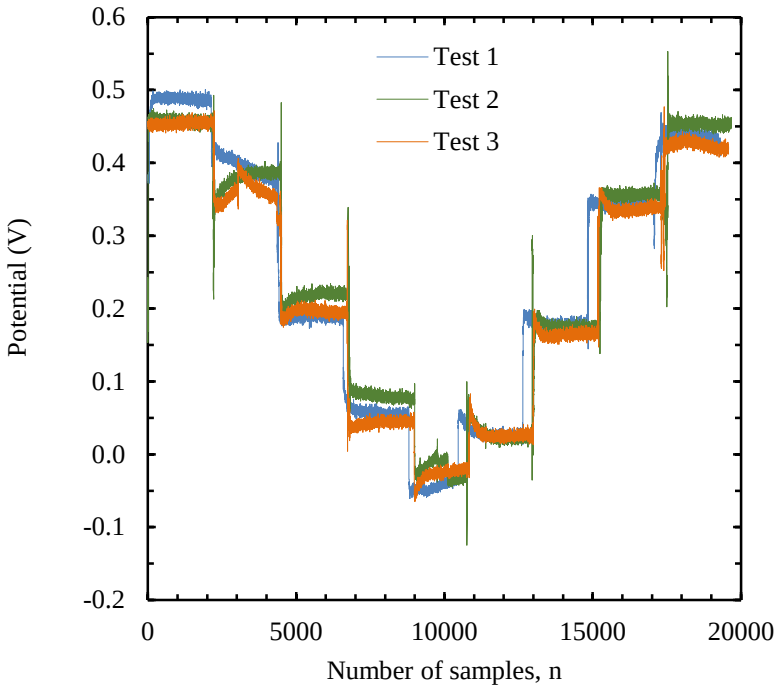

Figure 45: Reversibility and repeatability test performed on Al-IROF pH sensor with the pH testing sequence 1.936 – 11.698 – 1.936

5.3.6 *Reversibility and repeatability test on Ti-Al-IROF based pH sensor*

The sensor was able to detect 5 different pH solutions from 1.936 to 11.698 and showed reversibility when tested in the decreasing order of pH. The graph in the following figure shows the test for reversibility and repeatability.

We can see from the figure that the sensors are fairly reversible and repeatable.

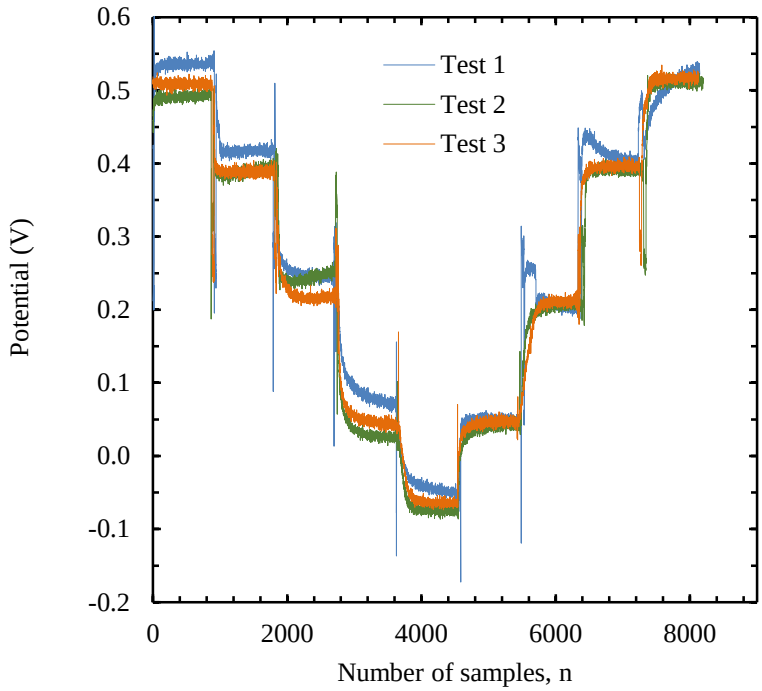

Figure 46: Reversibility and repeatability test performed on Ti-Al-IROF pH sensor with the pH testing sequence 1.936 – 11.698 – 1.936

5.3.7 *Reversibility and repeatability test on Cr-Au-IROF based pH sensor*

The sensor was able to detect 5 different pH solutions from 1.936 to 11.698 and showed reversibility when tested in the decreasing order of pH. The graph in the following figure shows the test for reversibility and repeatability.

We can see from the figure that the sensors are fairly reversible and repeatable.

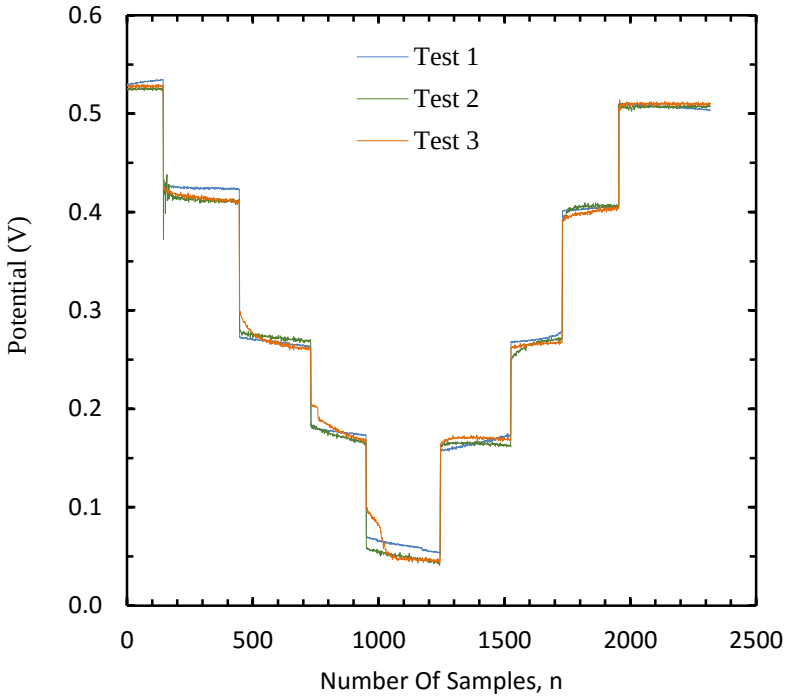

Figure 47: Reversibility and repeatability test performed on Cr-Au-IROF pH sensor with the pH testing sequence 1.936 – 11.698 – 1.936.

5.4 Performance evaluation and comparison of different sensors

As discussed above we need to consider different performance parameters to judge the ability of a particular sensor to sense the pH variations. The parameters have been tabulated in table 2. We have taken into account the sensitivity, potential drift, potential fluctuations, hysteresis and potential deviation. Also, the pH range in which a particular sensor works is also shown. When the sensor is introduced into a pH solution a peak in potential is observed which slowly reduces to attain a stable value. We define potential drift as difference between the peak potential value reached when introduced into a solution and 90% of the equilibrium potential.

We took an average of potential drift from different pH buffers and also over different readings which resulted in average potential drift.

Potential deviation is the variation in the stable value of the potential over different readings and different pH solutions. We took an average of potential deviation from different pH buffers and also over different readings which resulted in average potential deviation.

Average sensitivity can be defined as the average of sensitivities from different readings for a particular type of sensor.

Potential fluctuation is defined as the variation in the potential between the sensor and reference electrode when placed in a pH solution after reaching a stable value. This variation is expected to be small for good functioning of the pH sensor because after reaching a stable value if the variation is too high then it is difficult to discern the pH of the solution accurately. Average potential fluctuation is therefore defined as the average of potential fluctuations from different pH buffers and also over different readings.

Hysteresis is the next performance evaluating parameter. During reversibility test, we test a sensor for a particular pH value twice because we initially test the sensor in the increasing pH values and then in the decreasing order of pH values during one reading. So, we obtain two different potentials for the same pH in the course of the measurement. It is expected that, for an ideal sensor, these two potentials are the same. But in real case there is a little variation between these two values. This difference is called hysteresis. Average hysteresis is therefore defined as the average of hysteresis from different pH buffers and also over different readings.

From table 2 we can talk about the performance of the sensor based on different parameters and their values.

Type of sensor	Sensitive in the pH range	Sensitivity	Avg. Hysteresis (*dV*)	Avg. Potential Fluctuation (ΔV)	Avg. Potential Deviation (δ V)	Avg. Potential Drift (V')
Ni-IROF	4 to 10	59.17 mV/pH	4.1 mV	16.2 mV	12.25 mV	14.96 mV
Cr-Ni-IROF	4 to 10	55.9 mV/pH	5.02 mV	24.73 mV	12.22 mV	12.44 mV
Ti-Ni-IROF	4 to 10	53.67 mV/pH	2.42 mV	17 mV	12.77 mV	11.64 mV
C-Ni-IROF	4 to 10	46.05 mV/pH	6.135 mV	3.317 mV	14.26 mV	11.98 mV
Al-IROF	2 to 12	50.87 mV/pH	29.69 mV	25.8 mV	18.595 mV	23.062 mV
Ti-Al-IROF	2 to 12	60.03 mV/pH	25.396 mV	24.147 mV	22.964 mV	25.414 mV
Cr-Au-IROF	2 to 12	45.15 mV/pH	4.42 mV	6.28 mV	10.2 mV	8.5 mV

Table 2: Performance evaluating parameters of different pH sensors and their comparison

5.5 Discussion

First, let us compare the Ni based sensors. The Ni based sensors have shown sensitivities in a varied range from as high as 59.17 mV/pH for Ni-IROF pH sensor to 46.05 mV/pH for C-Ni-

IROF pH sensor. Adding an adhesion layer reduced the sensitivity of the sensors and in the order of decreasing sensitivities stand Cr, Ti and then a layer of sputtered carbon as the adhesion layers. All of these pH sensors were sensitive in pH range of 4 to 10.

Ni based sensors showed really low hysteresis which is good when used as a pH sensor because the sensors would be more reliable. The hysteresis was found to be in the range of 2 to 6 mV and was different for different adhesion layers. Introducing an adhesion layer of Ti showed low hysteresis of around 2.42 mV and introducing a layer of sputtered carbon before depositing Ni to form C-Ni-IROF pH sensor increased the hysteresis to 6.135 mV. But the Ni based pH sensors have very low hysteresis compared to Al and Au based pH sensors.

Coming to the parameter called potential fluctuations, we see that all the Ni based sensors have average potential fluctuations when compared to Al based pH sensors with the exception of C-Ni-IROF pH sensor which had a potential fluctuation value of 3.317 mV which is less than Au based pH sensor and it is also the lowest of the sensors. This means that the fluctuations after stabilization are very low which means that it easy to discern the pH values.

The next parameter that we will discuss is the potential deviation. For Ni based pH sensors the potential deviation is approximately the same. This value is lower when compared to Al based sensors and higher when compared to the Au based sensor. For optimal performance we want the value of the potential deviation to be minimum.

Finally, we discuss about the potential drift for the Ni based sensors. The potential drift is low for all the Ni based sensors and are comparably similar to that of Au based sensors.

Let us now compare the Al based sensors. The Al based sensors have shown high sensitivity values of 50.87 mV/pH for Al-IROF pH sensor and 60.03 mV/pH for Ti-Al-IROF pH sensor. Adding an adhesion layer increased the sensitivity of the sensors by approximately 10 mV/pH. All of these pH sensors were sensitive in pH range of 2 to 12 which is the main advantage of using Al based sensors over Ni based sensors.

Al based sensors showed higher hysteresis when used as a pH sensor when compared to Ni based sensors but lower than Au based sensors. The hysteresis was found to be in the range of 25 to 30 mV. Introducing an adhesion layer of Ti showed lower hysteresis but the difference is not significant.

Coming to the parameter called potential fluctuations, we see that all the Al based sensors have higher potential fluctuations when compared to Ni and Au based pH sensors. This means that the fluctuations after stabilization are high and that it is difficult to discern the pH values easily.

The next parameter that we will discuss is the potential deviation. For Al based pH sensors the potential deviation is approximately the same. This value is higher when compared to all other pH sensors. For optimal performance we want the value of the potential deviation to be minimum.

Finally, we discuss about the potential drift for the Al based sensors. The potential drift is very high for all the Al based sensors which is not desirable for a good performance.

5.6 Conclusion

In conclusion we can say many things about the devices that have been fabricated in this work. All Ni based sensors are functional in a very narrow pH range which means that they can be used in applications where the pH range is known to be in the range of 4 to 10 beforehand. But in this range their performance is good and is comparable to the Au based pH sensor. The Ni based sensors not only have good sensitivities but also have optimal performance parameters. Most importantly, the C-Ni-IROF based pH sensor has low sensitivity when compared to other Ni based pH sensors but it has a very low value of potential fluctuations which means that the performance can be better. The Ti-Ni-IROF pH sensor has a very low hysteresis which is good for repeatability of the device.

The Al based sensors have a wide pH range of 2 to 12 but the performance is low when compared to Ni based sensors. They have high value of potential fluctuation and hysteresis which is not good for accurate sensing and repeatability. Hence, the Al based sensors can be used in cases where we need to use a low cost sensor for broad range of pH values and when accuracy is not that important.

The Au based sensor is apt to use in pH sensing applications with a wide range and good performance.

REFERENCES

[1] A. Beckman, et al., "Apparatus for testing acidity", US2058761, 1936.

[2] John G. Webster, "The measurement, instrumentation and sensors handbook," CRC Press and IEEE Press, pp. 71-1, Florida, 1999.

[3] Otto S. Wolfbeis, "Fiber-optic chemical sensors and biosensors," Anal. Chem., Vol. 76,pp. 3269-3284, 2004.

[4] Sheila A. Grant, Robert S. Glass, "A sol-gel based fiber optic sensor for local blood pH measurements," Sensors and Actuators B, Vol. 45, pp. 35-42, 1997.

[5] Saying Dong, Ming Luo, Gangding Peng, and Wenhua Cheng, "Broad range pH sensor based on sol–gel entrapped indicators on fiber optic," Sensor and Actuators B: Chem. Vol.129, pp. 94-98, Jan., 2008.

[6] Zhe Jin, Yongxuan Su, and Yixiang Duan, "An improved optical pH sensor based on polyaniline," Sensors and Actuators B, Vol. 71, pp. 118-122, Nov., 2000.

[7] Afsaneh Safavi, Mozhgan, "Novel optical pH sensor for high and low pH values, “Sensors and Actuators B, Vol. 90, pp. 143-150, April, 2003.

[8] E.Alvarado-Mendez, R. Rojas-Laguna, J.A. Andrade-Lucio, D. Hernandez-Cruz, R.A. Lessard, and J.G. Avina-Cervantes, "Design and characterization of pH sensor based on sol–gel silica layer on plastic optical fiber," Sensors and Actuators B, Vol. 106, pp.518-522, May, 2005.

[9] Agner Fog, and Richard P. Buck, "Electronic semiconducting oxides as pH sensors," Sensors and Actuators, Vol. 6, pp. 137-146, 1984.

[10] T. Mikolajick, R. Kuhnhold, and H. Ryssel, "The pH-sensing properties of tantalum pentoxide films fabricated by metal organic low pressure chemical vapor deposition, "Sensors and Actuators B, Vol. 44, pp. 262-267, 1997.

[11] Patrick J. Kinlen, John E. Heider, and David E. Hubbard, "A solid-state pH sensor based on a Nafion-coated iridium oxide indicator electrode and a polymer-based silver chloride reference electrode," Sensors and Actuators B, Vol. 22, pp. 13-25, Oct., 1994.

[12] H. Neil McMurray, Peter Douglas, and Cuncan Abbot, "Novel thick-film pH sensors based on ruthenium dioxide-glass composites," Sensors and Actuators B, Vol. 28, pp. 9-15, July, 1995.

[13] Norman F. Sheppard, Jr., Matthew J. Lesho, Philip McNally, and A. Shaun Francomacaro, "Microfabricated conductimetric pH sensor," Sensors and Actuators B, Vol. 28, pp. 95-102, Aug., 1995.

[14] Gerald Gerlach, Margarita Guenther, Joerg Sorber, Gunnar Suchaneck, Karl-Friedrich Arndt, and Andreas Richter, "Chemical and pH sensors based on the swelling behavior of hydrogels," Sensors and Actuators B, Vol. 111-112, pp. 555-561, Nov., 2005.

[15] R.Bashir, J.Z. Hilt, O.Elibol, A.Gupta and N.A. Peppas, "Micromechanical cantilever as an ultrasensitive pH microsensor," Applied Physics Letters, Vol. 81, pp. 3091-3093, 2002.

[16] Young-Jin Kim, Young-Chul Lee, Byung-Ki Sohn, Jung-Hee Lee, and Chang-Soo Kim,"A novel pH microsensor with a built-in reference electrode," Journal of the Korean Physical Society, Vol. 43, pp. 769-772, 2003.

[17] Yi Liu, Tianhoung Cui, "Ion-sensitive field-effect transistor based pH sensors using nano self-assembled polyelectrolyte/nanoparticle multilayer films," Sensors and Actuators B, Vol. 123, pp. 148-152, Aug., 2006.

[18] Jinghong Han, Dafu Cui, Yating Li, Hong Zhang, Yuzi Huang, Zipan Zheng, Yaming Zhu and Xiangming Li, "A gastroesophageal tract pH sensor based on the H-ISFET and the monitoring system for 24 h," Sensors and Actuators B, Vol. 66, pp. 203-204, July, 2000.

[19] Kalman Pasztor, A. Sekiguchi, N. Shimo, N. Kitamura and H. Masuhara, "Iridium oxide-based micro electrochemical transistors for pH sensing," Sensors and Actuators B, Vol. 12, pp. 225-230, 1993.

[20] Huang, W., Cao, H., Deb, S., Chiao, M., & Chiao, J. C. (2011). “A flexible pH sensor based on the iridium oxide sensing film,” Sensors & Actuators: A. Physical, 169(1), 1-11. doi:10.1016/j.sna, 2011.

[21] Sheng Yao, Min Wang, and Marc Madou, "A pH electrode based on melt-oxidized iridium oxide," Journal of the Electrochemical Society, Vol. 148, pp. 29-36, 2001.

[22] Chu-Neng Tsai, Jung-Chuan Chou, Tai-Ping Sun, and Shen-Kan Hsiung, "Study on the sensing characteristics and hysteresis effect of the tin oxide pH electrode," Sensors and Actuators B, Vol. 18, pp. 877-882, July, 2005.

[23] Yi-Hung Liao and Jung-Chuan Chou, "Preparation and characteristics of ruthenium dioxide for pH array sensors with real-time measurement system," Sensor and Actuators B, Vol.128, pp. 603-612, Jan., 2007.

[24] J. V. Dobson, P. R. Snodin and H. R. Thirsk, "EMF measurements of cells employing metal-metal oxide electrodes in aqueous chloride and sulphate electrolytes at temperatures between 25–250°C," Electrochemical Acta, Vol. 21, pp. 527-533, 1976.

[25] C. Jefferey Brinker, George W. Scherer, "Sol-gel science: The physics and chemistry of sol-gel processing," Academic Press, pp. 788-798, Boston, 1990.

[26] M. Pourbaix, "Atlas of electrochemical equilibria in aqueous solutions," National Association of Corrosion Engineers, 1974.

[27] Jiang-Tsu, and Ying-Sheng Huang, "Electron paramagnetic resonance of a molecular defect in γ-irradiated IrO2 single crystals," Physical Review B, Vol. 40, pp. 4281-4288, 1989.

[28] Akiyoshi Osaka, Toru Takatsuna, and Yoshinari Miura, "Iridium oxide films via sol-gel processing," Non-Crystalline Solids, Vol. 178, pp. 313-319, 1994.

[29] Kazusuke Yamanaka, "Anodically electrodeposited iridium oxide films (AIROF) from alkaline solutions for electrochromic display devices," Japanese Journal of Applied Physics, Vol. 28, pp. 632-637, 1989.

[30] Michael L. Hitchman, and Subramaniam Ramanathan, "A field-induced poising technique for promoting convergence of standard electrode potential values of thermally oxidized iridium pH sensors," Talanta, Vol. 39, pp. 137-144, 1992.

[31] Keishi Nishio and Toshio Tsuchiya, "Electrochromic thin films prepared by sol-gel process," Solar Energy Materials& Solar Cells, Vol. 68, pp. 279-293, 2001.

[32] C. Jefferey Brinker, George W. Scherer, "Sol-gel science: The physics and chemistry of sol-gel processing, " Academic Press, pp. 788-798, Boston, 1990.

[33] M. Pourbaix, "Atlas of electrochemical equilibria in aqueous solutions," National Association of Corrosion Engineers, pp. 374-377, 1974.

[34] Erno Pungor, "The theory of ion-selective electrodes," Analytical Sciences. Vol. 14, pp. 249-256, 1998.

[35] Ges, I.A., Ivanov, B.L., Schaffer, D.K., Lima, E.A., Werdich, A.A. & Baudenbacher, F.J., "Thin-film IrOx pH microelectrode for microfluidic-based microsystems", Biosensors & bioelectronics, vol. 21, no. 2, pp. 248, 2005.

[36] Marzouk SAM, "Improved electrodeposited iridium oxide pH sensor fabricated on etched titanium substrates," Analytical chemistry, pp.1258-1266, 2005

[37] Marzouk, S. A., S. Ufer, R. P. Buck, et al. "Electrodeposited Iridium Oxide pH Electrode for Measurement of Extracellular Myocardial Acidosis during Acute Ischemia," Analytical Chemistry, vol. 70/no. 23, pp. 5054-5061, 1998

[38] Ges IA, Ivanov BL, Werdich AA, Baudenbacher FJ. "Differential pH measurements of metabolic cellular activity in nl culture volumes using micro fabricated iridium oxide electrodes," Biosensors and Bioelectronics, pp.22:1303-1310, 2007

[39] Saeid Kakooei, Mokhtar Che Ismail, Bambang Ari-Wahjoediz, "An overview of pH Sensors Based on Iridium Oxide: Fabrication and Application," International Journal of Material Science Innovations, pp. 62-72, 2013

[40] C. M. Nguyen, H.C., W. D. Huang, and J.-C. Chiao, An Electro-Deposited IrOx Thin Film pH Sensor, in BMES Biomedical Engineering Society Annual Meeting: Hartford, 2011.

[41] Huang W, Cao H, Deb S, Chiao M, Chiao JC. "A flexible pH sensor based on the iridium oxide sensing film," Sensors & Actuators: A. Physical, pp.1-11, 2011

[42] Huang, Wen-Ding, “A pH Sensor Based on A Flexible Substrate,” (Electrical Engineering, 2014, The University of Texas at Arlington)

[43] A.W.J.Cranny, J. K. Atkinson, "Thick film silver–silver chloride reference electrodes," Meas. Sci Technol, pp. 1557-1565, 1998.

[44] L.D. Burke, M.E. Lyons, E.J.M. O'Sullivan, and D.P. Whelan, "Influence of hydrolysis on the redox behavior of hydrous oxide films," J. Electroanal. Chem., Vol. 122, pp. 403-407, 1981.

[45] W. Olthuis, M. A. M. Robben, P. Bergveld, M. Bos and, W. E. van der Linden, "pH sensor properties of electrochemically grown iridium oxide," Sensor and Actuators B, Vol. 2, pp. 247-256, 1990.

BIOGRAPHICAL INFORMATION

Pavan Kumar Kota was born in Hyderabad, India. He received his bachelors' degree in Electronics and Communication Engineering from Shanmugha Arts, Science, Technology & Research Academy (SASTRA) University, Thanjavur, India in 2013. He received his Master of Science in Electrical Engineering from The University of Texas at Arlington in May 2016. His research interests include MEMS and sensors for biomedical applications.